

Quasi-Steady Flight to Quasi-Steady Flight Transition for Abort Landing in a Windshear: Trajectory Optimization and Guidance^{1,2}

A. MIELE,³ T. WANG,⁴ AND W. W. MELVIN⁵

Abstract. This paper is concerned with the optimal transition and the near-optimum guidance of an aircraft from quasi-steady flight to quasi-steady flight in a windshear. The abort landing problem is considered with reference to flight in a vertical plane. In addition to the horizontal shear, the presence of a downdraft is considered.

It is assumed that a transition from descending flight to ascending flight is desired; that the initial state corresponds to quasi-steady flight with absolute path inclination of -3.0 deg; and that the final path inclination corresponds to quasi-steady steepest climb. Also, it is assumed that, as soon as the shear is detected, the power setting is increased at a constant time rate until maximum power setting is reached; afterward, the power setting is held constant. Hence, the only control is the angle of attack. Inequality constraints are imposed on both the angle of attack and its time derivative.

First, trajectory optimization is considered. The optimal transition problem is formulated as a Chebyshev problem of optimal control: the performance index being minimized is the peak value of the modulus of the difference between the instantaneous altitude and a reference value, assumed constant. By suitable transformations, the Chebyshev problem is converted into a Bolza problem. Then, the Bolza problem is solved employing the dual sequential gradient-restoration algorithm (DSGRA) for optimal control problems.

Two types of optimal trajectories are studied, depending on the conditions desired at the final point. Type 1 is concerned with gamma

¹ This research was supported by NASA Langley Research Center, Grant No. NAG-1-516, by Boeing Commercial Airplane Company, and by Air Line Pilots Association.

² The authors are indebted to Dr. R. L. Bowles (NASA-LRC) and Dr. G. R. Hennig (BCAC) for helpful discussions.

³ Professor of Aerospace Sciences and Mathematical Sciences, Aero-Astronautics Group, Rice University, Houston, Texas.

⁴ Senior Research Scientist, Aero-Astronautics Group, Rice University, Houston, Texas.

⁵ Captain, Delta Airlines, Atlanta, Georgia; and Chairman, Airworthiness and Performance Committee, Air Line Pilots Association (ALPA), Washington, D.C.

recovery (recovery of the value of the relative path inclination corresponding to quasi-steady steepest climb). Type 2 is concerned with quasi-steady flight recovery (recovery of the values of the relative path inclination, the relative velocity, and the relative angle of attack corresponding to quasi-steady steepest climb). Both the Type 1 trajectory and the Type 2 trajectory include three branches: descending flight, nearly horizontal flight, and ascending flight. Also, for both the Type 1 trajectory and the Type 2 trajectory, descending flight takes place in the shear portion of the trajectory; horizontal flight takes place partly in the shear portion and partly in the aftershear portion of the trajectory; and ascending flight takes place in the aftershear portion of the trajectory. While the Type 1 trajectory and the Type 2 trajectory are nearly the same in the shear portion, they diverge to a considerable degree in the aftershear portion of the trajectory.

Next, trajectory guidance is considered. Two guidance schemes are developed so as to achieve near-optimum transition from quasi-steady descending flight to quasi-steady ascending flight: acceleration guidance (based on the relative acceleration) and gamma guidance (based on the absolute path inclination).

The guidance schemes for quasi-steady flight recovery in abort landing include two parts in sequence: shear guidance and aftershear guidance. The shear guidance is based on the result that the shear portion of the trajectory depends only mildly on the boundary conditions. Therefore, any of the guidance schemes already developed for Type 1 trajectories can be employed for Type 2 trajectories (descent guidance followed by recovery guidance). The aftershear guidance is based on the result that the aftershear portion of the trajectory depends strongly on the boundary conditions; therefore, the guidance schemes developed for Type 1 trajectories cannot be employed for Type 2 trajectories. For Type 2 trajectories, the aftershear guidance includes level flight guidance followed by ascent guidance. The level flight guidance is designed to achieve almost complete velocity recovery; the ascent guidance is designed to achieve the desired final quasi-steady state.

The numerical results show that the guidance schemes for quasi-steady flight recovery yield a transition from quasi-steady flight to quasi-steady flight which is close to that of the optimal trajectory, allows the aircraft to achieve the final quasi-steady state, and has good stability properties.

Key Words. Flight mechanics, abort landing, quasi-steady flight to quasi-steady flight transition, optimal trajectories, optimal control, guidance strategies, acceleration guidance, gamma guidance, feedback control, windshear problems, sequential gradient-restoration algorithm, dual sequential gradient-restoration algorithm.

1. Introduction

Low-altitude windshear is a threat to the safety of aircraft in take-off and landing (Ref. 1). Over the past 20 years, some 30 aircraft accidents have been attributed to windshear. The most notorious ones are the crash of PANAM Flight 759 on July 9, 1982 at New Orleans International Airport (Boeing B-727 in take-off, Ref. 2) and the crash of Delta Airlines Flight 191 on August 2, 1985 at Dallas-Fort Worth International Airport (Lockheed L-1011 in landing, Refs. 3-5).

Low-altitude windshear is usually associated with a severe meteorological phenomenon, called the downburst. In turn, a downburst involves a descending column of air, which then spreads horizontally in the neighborhood of the ground. This condition is hazardous, because an aircraft in take-off or landing might encounter a headwind coupled with a downdraft, followed by a tailwind coupled with a downdraft. The transition from headwind to tailwind engenders a transport acceleration, and hence a windshear inertia force (the product of the transport acceleration and the mass of the aircraft). In turn, the windshear inertia force can be as large as the drag of the aircraft, and in some cases as large as the thrust of the engines. Hence, an inadvertent encounter with a low-altitude windshear can be a serious problem for even a skilled pilot.

This paper is concerned with the landing problem. When the pilot of an aircraft on a glide path detects an inadvertent encounter with a low-altitude windshear, he has two choices: (i) penetration landing or (ii) abort landing. Clearly, if the initial altitude is high enough, abort landing is a safer procedure than penetration landing. In this connection, we note that a constant pitch guidance scheme for executing the abort landing maneuver was introduced and discussed in Refs. 6-8.

For the abort landing problem, optimal trajectories (trajectories minimizing the peak value of the altitude drop) were studied in Ref. 9. For the same problem, guidance trajectories approximating the optimal trajectories were studied in Refs. 10-11. Specifically, the following guidance schemes were developed in Refs. 10-11: (a) target altitude guidance, in which the target altitude is slightly above the minimum altitude of the optimal trajectory, Ref. 10; (b) safe target altitude guidance, in which the target altitude is slightly above the minimum altitude of the optimal trajectory for $\Delta W_x = 140 \text{ ft sec}^{-1}$, Ref. 10; (c) acceleration guidance, based on the relative acceleration, Ref. 11; (d) gamma guidance, based on the absolute path inclination, Ref. 11; and (e) modified constant pitch guidance, based on two target pitches, one to be used for descending flight and one to be used for horizontal flight/climbing flight, Ref. 11. For guidance schemes (c), (d), (e), the target altitude depends on the initial altitude and the

windshear intensity; these guidance schemes are characterized by descending flight before the target altitude is reached and horizontal flight/climbing flight after the target altitude is reached.

It must be noted that the optimal trajectories of Ref. 9 are designed to achieve gamma recovery (final value of the relative path inclination equal to that for quasi-steady steepest climb). Consistently with Ref. 9, the guidance trajectories of Refs. 10-11 are designed to achieve almost gamma recovery (final value of the relative path inclination nearly equal to that for quasi-steady steepest climb).

A more ambitious optimization undertaking is to design optimal abort landing trajectories which achieve quasi-steady flight recovery (final values of the relative velocity, the relative path inclination, and the relative angle of attack equal to those for quasi-steady steepest climb). Consistently, a more ambitious guidance undertaking is to design guidance trajectories which achieve almost quasi-steady flight recovery (final values of the relative velocity, the relative path inclination, and the relative angle of attack nearly equal to those for quasi-steady steepest climb). This is precisely the main objective of this paper. Attention is also devoted to the stability of the quasi-steady flight, meaning that the quasi-steady flight can be maintained after it is reached.

We close the introduction by noting that the present paper is part of a comprehensive research program undertaken at Rice University on optimal trajectories, guidance schemes, and piloting strategies for take-off, abort landing, and penetration landing. For previous studies of optimal trajectories and guidance schemes, see Refs. 9-20 and references therein.

2. Notations

Throughout the paper, the following notations are employed:

C_D = drag coefficient;

C_L = lift coefficient;

D = drag force, lb;

g = acceleration of gravity, ft sec⁻²;

h = altitude, ft;

K = gain coefficient, dimensionless or dimensional, depending on the feedback control law;

L = lift force, lb;

m = mass, lb ft⁻¹ sec²;

S = reference surface area, ft²;

t = time, sec;

T = thrust force, lb;

V = relative velocity, ft sec⁻¹;

- V_e = absolute velocity, ft sec⁻¹;
- $W = mg$ = weight, lb;
- W_h = h -component of wind velocity, ft sec⁻¹;
- W_x = x -component of wind velocity, ft sec⁻¹;
- x = horizontal distance, ft;
- α = relative angle of attack (wing), rad;
- α_e = absolute angle of attack (wing), rad;
- β = engine power setting;
- γ = relative path inclination, rad;
- γ_e = absolute path inclination, rad;
- δ = thrust inclination, rad;
- θ = pitch attitude angle (wing), rad;
- λ = wind intensity parameter;
- ρ = air density, lb ft⁻⁴ sec²;
- τ = final time, sec.

3. Equations of Motion

In this paper, we make use of the relative wind-axes system in connection with the following assumptions: (a) the aircraft is a particle of constant mass; (b) flight takes place in a vertical plane; (c) Newton's law is valid in an Earth-fixed system; (d) the wind flow field is steady; (e) at the windshear onset, the power setting is increased at a constant time rate until maximum power setting is reached; afterward, the power setting is held constant.

With the above premises, the equations of motion include the kinematical equations

$$\dot{x} = V \cos \gamma + W_x, \tag{1a}$$

$$\dot{h} = V \sin \gamma + W_h, \tag{1b}$$

and the dynamical equations

$$\begin{aligned} \dot{V} = & (T/m) \cos(\alpha + \delta) - D/m - g \sin \gamma \\ & - (\dot{W}_x \cos \gamma + \dot{W}_h \sin \gamma), \end{aligned} \tag{2a}$$

$$\begin{aligned} \dot{\gamma} = & (T/mV) \sin(\alpha + \delta) + L/mV - (g/V) \cos \gamma \\ & + (1/V)(\dot{W}_x \sin \gamma - \dot{W}_h \cos \gamma). \end{aligned} \tag{2b}$$

Because of assumption (d), the total derivatives of the wind velocity components and the corresponding partial derivatives satisfy the relations

$$\dot{W}_x = (\partial W_x / \partial x)(V \cos \gamma + W_x) + (\partial W_x / \partial h)(V \sin \gamma + W_h), \tag{3a}$$

$$\dot{W}_h = (\partial W_h / \partial x)(V \cos \gamma + W_x) + (\partial W_h / \partial h)(V \sin \gamma + W_h). \tag{3b}$$

These equations must be supplemented by the functional relations

$$T = T(h, V, \beta), \quad (4a)$$

$$D = D(h, V, \alpha), \quad L = L(h, V, \alpha), \quad (4b)$$

$$W_x = W_x(x, h), \quad W_h = W_h(x, h), \quad (4c)$$

and by the analytical relations

$$V_{ex} = V \cos \gamma + W_x, \quad V_{eh} = V \sin \gamma + W_h, \quad (5a)$$

$$V_e = \sqrt{(V_{ex}^2 + V_{eh}^2)}, \quad \gamma_e = \arctan(V_{eh}/V_{ex}), \quad (5b)$$

$$\theta = \alpha + \gamma, \quad \alpha_e = \alpha + \gamma - \gamma_e. \quad (5c)$$

For a given value of the thrust inclination δ , the differential system (1)–(4) involves four state variables [the horizontal distance $x(t)$, the altitude $h(t)$, the velocity $V(t)$, and the relative path inclination $\gamma(t)$] and two control variables [the angle of attack $\alpha(t)$ and the power setting $\beta(t)$]. However, the number of control variables reduces to one [the angle of attack $\alpha(t)$], if the power setting $\beta(t)$ is specified in advance [assumption (e)]. The quantities defined by the analytical relations (5) can be computed *a posteriori*, once the values of the state and the control are known.

Inequality Constraints. The angle of attack α and its time derivative $\dot{\alpha}$ are subject to the inequalities

$$\alpha \leq \alpha_*, \quad (6a)$$

$$-\dot{\alpha}_* \leq \dot{\alpha} \leq \dot{\alpha}_*, \quad (6b)$$

where α_* is a prescribed upper bound and $\dot{\alpha}_*$ is a prescribed, positive constant.

For the guidance schemes, Ineqs. (6) are enforced directly.

For the optimal trajectories, Ineqs. (6) are enforced indirectly via the following transformation technique:

$$\alpha = \alpha_* - u^2, \quad (7a)$$

$$\dot{u} = -(\dot{\alpha}_*/2u) \sin w, \quad |u| \geq \epsilon, \quad (7b)$$

$$\dot{u} = -(\dot{\alpha}_*/2u) \sin^2(\pi u/2\epsilon) \sin w, \quad |u| \leq \epsilon. \quad (7c)$$

Here, $u(t)$, $w(t)$ are auxiliary variables and ϵ is a small, positive constant, which is introduced to prevent the occurrence of boundary singularities. Note that the right-hand sides of Eqs. (7b)–(7c) are continuous and have continuous first derivatives at $|u| = \epsilon$. Clearly, when using Eqs. (7) in conjunction with Eqs. (1)–(4), one must regard $\alpha(t)$, $u(t)$ as state variables and $w(t)$ as control variable.

The power setting β and its time derivative $\dot{\beta}$ are subject to the inequalities

$$\beta_* \leq \beta \leq 1, \tag{8a}$$

$$-\dot{\beta}_* \leq \dot{\beta} \leq \dot{\beta}_*, \tag{8b}$$

where β_* is a prescribed lower bound and $\dot{\beta}_*$ is a prescribed, positive constant. The upper bound in (8a) means that, by definition, β is the ratio of the instantaneous thrust to the maximum thrust [see Eqs. (10)].

For both the optimal trajectories and the guidance schemes, Ineqs. (8) are enforced directly, since the power setting $\beta(t)$ is specified in advance. Indeed, because of assumption (e), the following relations hold:

$$\beta = \beta_0 + \dot{\beta}_0 t, \quad 0 \leq t \leq \sigma, \tag{9a}$$

$$\beta = 1, \quad \sigma \leq t \leq \tau, \tag{9b}$$

where

$$\sigma = (1 - \beta_0) / \dot{\beta}_0. \tag{9c}$$

Here, β_0 is the initial power setting, $\dot{\beta}_0$ is the constant time rate of increase of the power setting, σ is the time at which maximum power setting is reached, and τ is the final time.

4. System Description

The numerical examples of this paper refer to a Boeing B-727 aircraft powered by three JT8D-17 turbofan engines. It is assumed that: the runway is located at sea-level altitude; the ambient temperature is 100 deg F; the gear is down; the flap setting is $\delta_F = 30$ deg; the landing weight is $W = 150,000$ lb.

Thrust. The dependence of the thrust on the altitude is disregarded, and the function (4a) is written as

$$T = \beta T_*(V), \tag{10a}$$

$$T_* = A_0 + A_1 V + A_2 V^2. \tag{10b}$$

The reference thrust $T_*(V)$ is given in Fig. 1A. The power setting β is given by Eqs. (9), where β_0 is the initial power setting and $\dot{\beta}_0 = 0.2 \text{ sec}^{-1}$.

Aerodynamic Forces. The dependence of the drag and the lift on the altitude is disregarded, and the functions (4b) are written as

$$D = (1/2) C_D(\alpha) \rho S V^2, \tag{11a}$$

$$L = (1/2) C_L(\alpha) \rho S V^2, \tag{11b}$$

with

$$C_D = B_0 + B_1\alpha + B_2\alpha^2, \quad \alpha \leq \alpha_*, \quad (12a)$$

$$C_L = C_0 + C_1\alpha, \quad \alpha \leq \alpha_{**}, \quad (12b)$$

$$C_L = C_0 + C_1\alpha + C_2(\alpha - \alpha_{**})^2, \quad \alpha_{**} \leq \alpha \leq \alpha_*. \quad (12c)$$

The drag coefficient $C_D(\alpha)$ is given in Fig. 1B, and the lift coefficient $C_L(\alpha)$ is given in Fig. 1C. The angle of attack α is subject to Ineqs. (6), with $\alpha_* = 17.2$ deg and $\dot{\alpha}_* = 3.0$ deg sec⁻¹.

Weight. Fuel consumption is neglected, and the weight $W = mg$ is regarded to be constant, $W = 150,000$ lb.

Wind Model. The dependence of the horizontal wind on the altitude is disregarded, and the functions (4c) are written as

$$W_x = \lambda A(x), \quad (13a)$$

$$W_h = \lambda (h/h_*) B(x), \quad (13b)$$

with

$$\lambda = \Delta W_x / \Delta W_{x*}. \quad (13c)$$

The function $A(x)$ represents the distribution of the horizontal wind versus the horizontal distance (Fig. 2); the function $B(x)$ represents the distribution of the vertical wind versus the horizontal distance (Fig. 2); the parameter λ characterizes the intensity of the shear/downdraft combination; ΔW_x is the horizontal wind velocity difference (maximum tailwind minus maximum headwind); $\Delta W_{x*} = 100$ ft sec⁻¹ is a reference value for the horizontal wind velocity difference; and $h_* = 1000$ ft is a reference value for the altitude.

The one-parameter family of wind models (13) has the following properties: (a) it represents the transition from a uniform headwind to a uniform tailwind, with nearly constant shear in the core of the downburst; (b) the downdraft achieves maximum negative value at the center of the downburst; (c) the downdraft vanishes at $h = 0$; and (d) the functions W_x , W_h nearly satisfy the continuity equation and the irrotationality condition in the core of the downburst. For previous literature on wind models, see Refs. 21-23.

Decreasing values of λ (hence, decreasing values of ΔW_x) correspond to milder windshears; conversely, increasing values of λ (hence, increasing values of ΔW_x) correspond to more severe windshears. If one excludes the 1983 windshear episode at Andrews AFB, the highest value of λ ever recorded is $\lambda = 1.40$, corresponding to $\Delta W_x = 140$ ft sec⁻¹. Hence, in this

paper, the following values of λ and ΔW_x are considered:

$$\lambda = 1.00, 1.20, 1.40, \tag{14a}$$

$$\Delta W_x = 100, 120, 140 \text{ ft sec}^{-1}. \tag{14b}$$

Initial Conditions. For the examples reported in this paper, the following initial conditions are assumed:

$$x_0 = 0 \text{ ft}, \tag{15a}$$

$$h_0 = 200, 600, 1000 \text{ ft}, \tag{15b}$$

$$V_0 = 142 \text{ knots} = 239.7 \text{ ft sec}^{-1}, \tag{15c}$$

$$\gamma_{e0} = -3.0 \text{ deg.} \tag{15d}$$

The initial velocity (15c) is FAA certification velocity V_{ref} augmented by 10 knots. The initial absolute path inclination (15d) is the standard glide slope used in the approach maneuver. The initial values $\gamma_0, \alpha_0, \beta_0$ are computed using (15) and the assumption of quasi-steady flight prior to the windshear onset. Therefore, they are computed by solving the nonlinear system

$$T \cos(\alpha + \delta) - D - W \sin \gamma = 0, \tag{16a}$$

$$T \sin(\alpha + \delta) + L - W \cos \gamma = 0, \tag{16b}$$

$$\tan \gamma_e - (V \sin \gamma + W_h)/(V \cos \gamma + W_x) = 0, \tag{16c}$$

in conjunction with Eqs. (10)-(13). The numerical solutions are given in Table 1 for several values of the wind intensity parameter λ .

Final Conditions. For the examples reported in this paper, the following final time is assumed:

$$\tau = 40 \text{ sec.} \tag{17}$$

The final time (17) is about twice the duration of the windshear encounter, $\Delta t = 22 \text{ sec.}$

The final values $V_\tau, \gamma_\tau, \alpha_\tau$ are computed using the assumption of quasi-steady state at maximum power setting. Therefore, they are computed by solving the nonlinear system

$$T \cos(\alpha + \delta) - D - W \sin \gamma = 0, \tag{18a}$$

$$T \sin(\alpha + \delta) + L - W \cos \gamma = 0, \tag{18b}$$

in conjunction with Eqs. (10)-(13) and $\beta = 1$. Since the system admits an infinite number of solutions, the solution is rendered unique by maximizing

the relative path inclination (steepest climb). Thus, one solves the mathematical programming problem

$$(Q) \max(\gamma), \quad \text{subject to Eqs. (18) and } \beta = 1. \quad (19)$$

The numerical solutions are given in Table 2 for several values of the wind intensity parameter λ .

5. Optimal Trajectories

We refer to abort landing and we assume that: global information on the wind flow field is available, that is, the functions (4c) are known in advance; the power setting $\beta(t)$ is given by Eqs. (9); and the angle of attack $\alpha(t)$ is subject to Ineqs. (6). Hence, upon converting the inequalities into equalities, we refer to the differential system described by Eqs. (1)–(4) and (7). In this system, the state variables are $x(t)$, $h(t)$, $V(t)$, $\gamma(t)$, $\alpha(t)$, $u(t)$ and the control variable is $w(t)$.

Concerning the boundary conditions, the following assumptions are employed:

- (i) the initial values $x(0)$, $h(0)$, $V(0)$, $\gamma(0)$, $\alpha(0)$, $u(0)$ are specified; see Eqs. (15) and Table 1;
- (ii) the final time τ is specified; see Eq. (17);
- (iii) either gamma recovery is desired, namely, the final value $\gamma(\tau)$ is given; or quasi-steady flight recovery is desired, namely, the final values $V(\tau)$, $\gamma(\tau)$, $\alpha(\tau)$, $u(\tau)$ are given; see Table 2.

With reference to (iii), the boundary conditions are said to be of Type 1 if gamma recovery is desired; they are said to be of Type 2 if quasi-steady flight recovery is desired.

With the above understanding, we formulate the following optimization problem.

Problem (P). Subject to the previous constraints, minimize the peak value of the altitude drop, that is, minimize the peak value of the modulus of the difference between a constant reference altitude and the instantaneous altitude. In this problem, the performance index is given by

$$I = \max_t |h_R - h|, \quad 0 \leq t \leq \tau. \quad (20a)$$

This is a minimax problem or Chebyshev problem of optimal control. By exploiting a well-known theorem of functional analysis, the Chebyshev

problem can be reformulated as a Bolza problem of optimal control, in which one minimizes the integral performance index

$$J = \int_0^{\tau} (h_R - h)^q dt, \quad (20b)$$

for large values of the positive, even exponent q (for instance, $q = 6$).

We note that the value of h_R must be selected with some care. Specifically, the difference $h_R - h$ should always be positive; however, for computational precision, excessively large values of h_R should be avoided.

The solution of Problem (P) for boundary conditions of Type 1 is called optimal trajectory OT1. The solution of Problem (P) for boundary conditions of Type 2 is called optimal trajectory OT2.

Sequential Gradient-Restoration Algorithm. Upon conversion of a Chebyshev problem into a Bolza problem, numerical solutions can be obtained by means of the sequential gradient-restoration algorithm (SGRA, Refs. 24–27), in either the primal formulation (PSGRA, Refs. 24–25) or the dual formulation (DSGRA, Refs. 26–27).

Regardless of whether the primal formulation is used or the dual formulation is used, sequential gradient-restoration algorithms involve a sequence of two-phase cycles, each cycle including a gradient phase and a restoration phase. In the gradient phase, the value of the augmented functional is decreased, while avoiding excessive constraint violation. In the restoration phase, the value of the constraint error is decreased, while avoiding excessive change in the value of the functional. In a complete gradient-restoration cycle, the value of the functional is decreased, while the constraints are satisfied to a preselected degree of accuracy. Thus, a succession of suboptimal solutions is generated, each new solution being an improvement over the previous one from the point of view of the value of the functional being minimized.

The convergence conditions are represented by the relations

$$P \leq \epsilon_1, \quad Q \leq \epsilon_2. \quad (21)$$

Here, P is the norm squared of the error in the constraints; Q is the norm squared of the error in the optimality conditions; and ϵ_1, ϵ_2 are preselected, small, positive numbers.

In this work, the sequential gradient-restoration algorithm is employed in conjunction with the dual formulation. The algorithmic details can be found in Refs. 26–27; they are omitted here, for the sake of brevity.

6. Numerical Results on Optimal Trajectories

Problem (P), $\text{minimax } |\Delta h|$, was solved with the sequential gradient-restoration algorithm, employed in conjunction with the dual formulation (DSGRA, Refs. 24–25). Computations were performed at Rice University using an NAS-AS-9000 computer.

Optimal trajectories OT1 and optimal trajectories OT2 were computed for several combinations of initial altitude and wind velocity difference, namely,

$$h_0 = 200, 600, 1000 \text{ ft}, \quad (22a)$$

$$\Delta W_x = 100, 120, 140 \text{ ft sec}^{-1}. \quad (22b)$$

The results are given in Tables 3–4 and Figs. 3–5.

Table 3 refers to the optimal trajectories OT1 and Table 4 refers to the optimal trajectories OT2. Each table exhibits the following quantities: the initial altitude h_0 , the wind velocity difference ΔW_x , the minimum altitude h_{\min} , the final altitude h_r , the final velocity V_r , the final path inclination γ_r , and the final angle of attack α_r .

Figure 3 shows the altitude distribution $h(t)$ for both the optimal trajectories OT1 and the optimal trajectories OT2 under the assumption that $h_0 = 600$ ft. This figure includes three parts: Fig. 3A refers to a strong windshear, $\Delta W_x = 100 \text{ ft sec}^{-1}$; Fig. 3B refers to a severe windshear, $\Delta W_x = 120 \text{ ft sec}^{-1}$; and Fig. 3C refers to an extremely severe windshear, $\Delta W_x = 140 \text{ ft sec}^{-1}$.

Figure 4 refers to the optimal trajectories OT1 and Fig. 5 refers to the optimal trajectories OT2, which are computed for $h_0 = 600$ ft and three values of the wind velocity difference [see (22b)]. Each figure includes four parts: the altitude distribution $h(t)$; the velocity distribution $V(t)$; the path inclination distribution $\gamma(t)$; and the angle of attack distribution $\alpha(t)$.

From Tables 3–4 and Figs. 3–5, the following facts can be inferred.

(F1) Both the OT1 and the OT2 include three branches in sequence: an initial branch, flown entirely in the shear portion of the trajectory; a central branch, flown partly in the shear portion and partly in the aftershear portion; and a final branch, flown entirely in the aftershear portion of the trajectory. For strong-to-severe windshears, the initial branch is descending, the central branch is nearly horizontal, and the final branch is ascending.

(F2) For the shear portion of the trajectory, the altitude distribution of the OT1 is nearly the same as the altitude distribution of the OT2.

(F3) For the aftershear portion of the trajectory, the altitude distribution of the OT1 diverges from the altitude distribution of the OT2. This is due to the fact that different final conditions must be met, namely, γ

recovery for the OT1 and quasi-steady flight recovery for the OT2. In particular, the final altitude of the OT2 is lower than the final altitude of the OT1, consistently with the fact that the final velocity of the OT2 is higher than the final velocity of the OT1.

With particular reference to the OT2 and to strong-to-severe windshears, the following additional comments can be made.

(C1) Altitude. The optimal trajectory OT2 includes three branches: descending flight, nearly horizontal flight, and ascending flight. The peak altitude drop depends on the initial altitude and the windshear intensity; it increases as the initial altitude increases and the windshear intensity increases.

(C2) Velocity. The velocity decreases in the shear portion of the trajectory and increases in the aftershear portion of the trajectory. The point of minimum velocity is achieved at the end of the shear. In the range of initial altitudes and windshear intensities given by (22), the minimum velocity is nearly independent of h_0 and ΔW_x ; also, the minimum velocity is near to (but is not equal to, because of dynamical effects and windshear effects) the stick-shaker velocity in quasi-steady level flight, $V_* = 179.3 \text{ ft sec}^{-1}$. In the neighborhood of the final point, the velocity is almost constant and equal to its final quasi-steady value.

(C3) Path Inclination. For the shear portion of the trajectory, the path inclination is negative in descending flight; then, it switches to a slightly positive value in nearly horizontal flight (to compensate for downdraft effects). For the aftershear portion of the trajectory, the path inclination is almost zero, while the velocity increases in nearly horizontal flight; then, the path inclination increases toward its final quasi-steady value, while the velocity is almost constant.

(C4) Angle of Attack. For the shear portion of the trajectory, the angle of attack exhibits an initial decrease, followed by a gradual, sustained increase; the peak value of the angle of attack is achieved near the end of the shear. For the aftershear portion of the trajectory, the angle of attack decreases as the velocity increases in nearly horizontal flight; in the neighborhood of the final point, a final adjustment in the angle of attack takes place, consistently with the need for recovering the final quasi-steady value of the path inclination.

7. Guidance Trajectories

In Sections 5-6, optimal trajectories were determined for two types of boundary conditions: optimal trajectories OT1 correspond to boundary

conditions of Type 1 (gamma recovery desired at the final point); optimal trajectories OT2 correspond to boundary conditions of Type 2 (quasi-steady flight recovery desired at the final point).

In this section, we discuss guidance trajectories GT1 and GT2 approximating the optimal trajectories OT1 and OT2, with the following understanding: while the optimal trajectories OT1 and OT2 rely on global information on the wind distribution, the guidance trajectories GT1 and GT2 rely on local information on the horizontal wind acceleration, the downdraft, and the state of the aircraft. For previous work on guidance trajectories GT1, see Refs. 10-11.

The following ideas are essential to the development of guidance trajectories GT2:

(A1) in an abort landing, the initial path inclination is descending and the final path inclination is ascending; hence, an abort landing trajectory can be viewed as a transition from descending flight to ascending flight;

(A2) if the abort landing maneuver is initiated at high altitude, containing the velocity loss should have priority over containing the altitude drop;

(A3) if the abort landing maneuver is initiated at low altitude, containing the altitude drop should have priority over containing the velocity loss.

Since the guidance trajectories GT2 must approximate the optimal trajectories OT2, the following additional considerations must be kept in mind:

(B1) both the OT1 and the OT2 include three branches in sequence: an initial branch, flown entirely in the shear portion of the trajectory; a central branch, flown partly in the shear portion and partly in the aftershear portion of the trajectory; and a final branch, flown entirely in the aftershear portion of the trajectory;

(B2) for strong-to-severe windshears, the initial branch is descending, the central branch is nearly horizontal, and the final branch is ascending;

(B3) the shear portion of the trajectory includes all of the descending flight branch and part of the horizontal flight branch; for the shear portion, the OT2 is nearly identical with the OT1; hence, the GT2 should be identical with the GT1;

(B4) the aftershear portion of the trajectory includes part of the horizontal flight branch and all of the ascending flight branch; for the aftershear portion, the OT2 diverges to a considerable degree from the OT1; hence, the GT2 should be different from the GT1; this means that a new guidance scheme must be developed;

(B5) with reference to the aftershear portion of the trajectory, the guidance scheme for the horizontal flight branch must be designed to achieve almost complete velocity recovery, while the path inclination is kept at nearly zero value; in this way, the behavior of the GT2 mirrors that of the OT2;

(B6) also with reference to the aftershear portion of the trajectory, the guidance scheme for the ascending flight branch must be designed to achieve almost complete restoration of the final quasi-steady state; hence, the path inclination must be increased from about zero value to the desired final value, while the velocity is kept nearly constant; in this way, the behavior of the GT2 mirrors that of the OT2.

With ideas (A1)-(A3) and considerations (B1)-(B6) in mind, we introduce in the following sections two guidance schemes: acceleration guidance (Section 8) and gamma guidance (Section 9). Then, numerical results for the guidance schemes are presented in Section 10. Finally, with reference to the final ascending branch, the stability properties of the guidance schemes are discussed in Section 11. There, a justification of the gain coefficients employed in Section 10 is given.

8. Acceleration Guidance

The acceleration guidance scheme includes a part pertaining to the shear portion of the trajectory (descent guidance followed by recovery guidance in nearly horizontal flight) and a part pertaining to the aftershear portion of the trajectory (level flight guidance followed by ascent guidance).

Shear Guidance. For the descent guidance, the key property is that the velocity is nearly constant, while the altitude decreases. Hence, the descent guidance law has the form

$$\dot{V}/g = 0. \quad (23)$$

For the recovery guidance in nearly horizontal flight, the key property is that the instantaneous acceleration is proportional to the shear/downdraft factor F , introduced in Ref. 12. Hence, the recovery guidance law has the form

$$\dot{V}/g + CF = 0, \quad (24a)$$

where C is a constant, having the typical value

$$C = 0.5. \quad (24b)$$

Note that the shear/downdraft factor is given by

$$F = (\dot{W}_x/g) \cos \gamma + (\dot{W}_h/g) \sin \gamma - W_h/V, \quad (24c)$$

which reduces to

$$F = \dot{W}_x/g - W_h/V, \quad (24d)$$

if the approximations

$$|\gamma| \ll 1 \quad \text{and} \quad |\dot{W}_h \gamma / \dot{W}_x| \ll 1 \quad (24e)$$

are employed.

Aftershear Guidance. For the level flight guidance, the key property is that the velocity increases, while the altitude is kept nearly constant. Hence, the level flight guidance law has the form

$$\dot{h} = 0, \quad (25)$$

where \dot{h} denotes the rate of climb.

For the ascent guidance, the key property is that the path inclination (hence, the rate of climb) increases toward its final value, while the velocity is kept nearly constant. Hence, the ascent guidance law has the form

$$\dot{h} - \dot{h}_\tau = 0, \quad (26)$$

where the subscript τ denotes the final point. Here, \dot{h}_τ is the rate of climb corresponding to steepest climb in quasi-steady flight.

Feedback Control. The guidance laws (23)–(26) can be implemented in the feedback control forms given below:

$$\alpha - \tilde{\alpha}(V) = K_1(\dot{V}/g - 0), \quad (27a)$$

$$\alpha - \tilde{\alpha}(V) = K_2[\dot{V}/g - (-CF)], \quad (27b)$$

$$\alpha - \tilde{\alpha}(V) = -K_3(\dot{h} - 0), \quad (27c)$$

$$\alpha - \tilde{\alpha}(V) = -K_4(\dot{h} - \dot{h}_\tau). \quad (27d)$$

Here, Eq. (27a) refers to the descent guidance; Eq. (27b) refers to the recovery guidance; Eq. (27c) refers to the level flight guidance; and Eq. (27d) refers to the ascent guidance.

In Eqs. (27), the angle of attack α is subject to the inequalities

$$\alpha \leq \alpha_*, \quad -\dot{\alpha}_* \leq \dot{\alpha} \leq \dot{\alpha}_*. \quad (28)$$

The symbol $\tilde{\alpha}(V)$ denotes the nominal angle of attack, whose conception is discussed in Ref. 12. The symbols K_i , $i=1, \dots, 4$, denote the gain

coefficients, having the following typical values (B-727 airplane):

$$K_1 = 10 \text{ rad}, \tag{29a}$$

$$K_2 = 10 \text{ rad}, \tag{29b}$$

$$K_3 = 0.005 \text{ rad ft}^{-1} \text{ sec}, \tag{29c}$$

$$K_4 = 0.005 \text{ rad ft}^{-1} \text{ sec}. \tag{29d}$$

Switch Criteria. In the acceleration guidance scheme, one must define (i) a switch criterion governing the transition from descent guidance to recovery guidance, (ii) a switch criterion governing the transition from recovery guidance to level flight guidance, and (iii) a switch criterion governing the transition from level flight guidance to ascent guidance.

With reference to (i), the transition from descent guidance to recovery guidance occurs when

$$h = h_T, \tag{30a}$$

that is, when the flight altitude is equal to a predetermined target altitude. In turn, the target altitude is given by (Ref. 11)

$$\begin{aligned} h_T &= 0.76h_0 + (0.336 - 1.70 \dot{W}_x/g)h_*, \\ 0.2h_* &\leq h_T \leq 0.9h_0, \end{aligned} \tag{30b}$$

and is such that

$$h_0 - h_T = 0.4(h_0 - h_{\min}). \tag{30c}$$

Here, h_{\min} denotes the minimum altitude of the optimal trajectory, given by

$$h_{\min} = 0.4h_0 + (0.84 - 4.25 \dot{W}_x/g)h_*, \quad 0 \leq h_{\min} \leq h_0. \tag{30d}$$

In Eqs. (30), the symbol $h_* = 1000 \text{ ft}$ denotes a reference altitude.

With reference to (ii), the transition from recovery guidance to level flight guidance occurs when the shear region is past and the velocity starts to increase; that is, it must be performed when the instantaneous acceleration \dot{V} switches from negative to positive.

With reference to (iii), the transition from level flight guidance to ascent guidance must be performed when the instantaneous velocity is within a certain tolerance of the final velocity. Hence, it must occur when

$$V = V_T, \tag{31a}$$

where the target velocity is given by

$$V_T = V_r - \Delta V, \tag{31b}$$

with

$$\Delta V = 6 \text{ ft sec}^{-1}. \quad (31c)$$

9. Gamma Guidance

As in the acceleration guidance scheme, the gamma guidance scheme includes a part pertaining to the shear portion of the trajectory (descent guidance followed by recovery guidance in nearly horizontal flight) and a part pertaining to the aftershear portion of the trajectory (level flight guidance followed by ascent guidance). While in the acceleration guidance scheme the recovery guidance and the level flight guidance are different, in the gamma guidance scheme they are the same. Hence, the switch criterion (ii) from recovery guidance to level flight guidance, which is needed in the acceleration guidance scheme, is not needed in the gamma guidance scheme.

Shear Guidance. For the descent guidance, the key property is that the absolute path inclination γ_e is negative; its average magnitude increases as the windshear intensity increases; therefore, it increases as the altitude drop associated with the optimal trajectory increases. The descent guidance law has the form

$$\gamma_e = \tilde{\gamma}_e, \quad (32a)$$

where $\tilde{\gamma}_e$ is the nominal absolute path inclination, given by

$$\tilde{\gamma}_e = -(h_0 - h_{min})/Eh_*, \quad \tilde{\gamma}_e \leq 0, \quad (32b)$$

with

$$E = 2.2 \quad (32c)$$

for the B-727 airplane. On account of Eq. (30d), Eq. (32b) can be rewritten as

$$\tilde{\gamma}_e = -(0.6h_0/h_* + 4.25\dot{W}_x/g - 0.84)/E, \quad \tilde{\gamma}_e \leq 0. \quad (32d)$$

For the recovery guidance in nearly horizontal flight, the key property is that the velocity decreases, while the absolute path inclination is about zero. Hence, the recovery guidance law has the form

$$\gamma_e = 0. \quad (33)$$

Aftershear Guidance. For the level flight guidance, the key property is that the velocity increases, while the absolute path inclination is nearly

zero. Hence, the level flight guidance law has the form

$$\gamma_e = 0, \tag{34}$$

which is identical with (33).

For the ascent guidance, the key property is that the path inclination increases toward its final value, while the velocity is kept nearly constant. Hence, the ascent guidance law has the form

$$\gamma_e = \gamma_{e\tau}, \tag{35}$$

where the subscript τ denotes the final point. Here, $\gamma_{e\tau}$ is the absolute path inclination corresponding to steepest climb in quasi-steady flight.

Feedback Control. The guidance laws (32)–(35) can be implemented in the feedback control forms given below:

$$\alpha - \tilde{\alpha}(V) = -K_1(\gamma_e - \tilde{\gamma}_e), \tag{36a}$$

$$\alpha - \tilde{\alpha}(V) = -K_2(\gamma_e - 0), \tag{36b}$$

$$\alpha - \tilde{\alpha}(V) = -K_3(\gamma_e - 0), \tag{36c}$$

$$\alpha - \tilde{\alpha}(V) = -K_4(\gamma_e - \gamma_{e\tau}). \tag{36d}$$

Here, Eq. (36a) refers to the descent guidance; Eq. (36b) refers to the recovery guidance; Eq. (36c) refers to the level flight guidance; and Eq. (36d) refers to the ascent guidance.

In Eqs. (36), the angle of attack α is subject to the inequalities

$$\alpha \leq \alpha_*, \quad -\dot{\alpha}_* \leq \dot{\alpha} \leq \dot{\alpha}_*. \tag{37}$$

The symbol $\tilde{\alpha}(V)$ denotes the nominal angle of attack, whose conception is discussed in Ref. 12. The symbols K_i , $i = 1, \dots, 4$, denote the gain coefficients having the following typical values (B-727 airplane)

$$K_1 = 1, \tag{38a}$$

$$K_2 = 1, \tag{38b}$$

$$K_3 = 1, \tag{38c}$$

$$K_4 = 2. \tag{38d}$$

Switch Criteria. In the gamma guidance scheme, one must define (i) a switch criterion governing the transition from descent guidance to recovery guidance and (iii) a switch criterion governing the transition from level flight guidance to ascent guidance. The switch criterion (ii), governing the transition from recovery guidance to level flight guidance, is not needed,

since the guidance laws (33) and (34) are identical; hence, the feedback control laws (36b) and (36c) are identical.

For the gamma guidance scheme, switch criterion (i) is identical with the corresponding switch criterion of the acceleration guidance scheme. Hence, Eqs. (30) apply.

For the gamma guidance scheme, switch criterion (iii) is identical with the corresponding switch criterion of the acceleration guidance scheme. Hence, Eqs. (31) apply.

10. Numerical Results on Guidance Trajectories

Using the data of Section 4, numerical results were obtained for the acceleration guidance scheme and the gamma guidance scheme. The acceleration guidance scheme was implemented in the feedback control form (27)-(29), with switch criteria supplied by (30)-(31). The gamma guidance scheme was implemented in the feedback control form (36)-(38), with switch criteria supplied by (30)-(31).

Several combinations of initial altitude and windshear intensity were considered, namely,

$$h_0 = 200, 600, 1000 \text{ ft}; \quad (39a)$$

$$\Delta W_x = 100, 120, 140 \text{ ft sec}^{-1}. \quad (39b)$$

For these combinations, the acceleration guidance trajectories AGT2 and the gamma guidance trajectories GGT2 were computed under the assumption that the initial conditions are supplied by Table 1 and the final conditions are supplied by Table 2. The numerical results are shown in Tables 5-6 and Figs. 6-7.

Table 5 refers to the acceleration guidance trajectories AGT2, and Table 6 refers to the gamma guidance trajectories GGT2. Each table exhibits the following quantities: the initial altitude h_0 , the wind velocity difference ΔW_x , the minimum altitude h_{\min} , the final altitude h_r , the final velocity V_r , the final path inclination γ_r , and the final angle of attack α_r .

Figure 6 refers to the acceleration guidance trajectories AGT2 and Fig. 7 refers to the gamma guidance trajectories GGT2, computed for $h_0 = 600$ ft and three values of the wind velocity difference [see (39b)]. Each figure includes four parts: the altitude distribution $h(t)$; the velocity distribution $V(t)$; the path inclination distribution $\gamma(t)$; and the angle of attack distribution $\alpha(t)$.

From the numerical solutions, upon comparing the acceleration guidance trajectories AGT2, the gamma guidance trajectories GGT2, and the optimal trajectories OT2, certain general conclusions became apparent.

(i) The function $h(t)$ of the AGT2 and the function $h(t)$ of the GGT2 are close to the function $h(t)$ of the OT2. The trajectories of both the AGT2 and the GGT2 include a descending branch, followed by a nearly horizontal branch, followed by an ascending branch, just as the OT2.

(ii) For both the AGT2 and the GGT2, the peak altitude drop depends on the initial altitude and the windshear intensity, increasing as the initial altitude and the windshear intensity increase. This property is consistent with the analogous property of the OT2.

(iii) The function $V(t)$ of the AGT2 and the function $V(t)$ of the GGT2 are close to the function $V(t)$ of the OT2. For both the AGT2 and the GGT2, the point of minimum velocity is achieved near the end of the shear ($t = 22$ sec). In the range of initial altitudes and windshear intensities considered, the minimum velocity is nearly independent of h_0 and ΔW_x . Also, the minimum velocity is near to (but is not equal to, because of dynamical effects and windshear effects) the stick-shaker velocity in quasi-steady level flight, $V_* = 179.3 \text{ ft sec}^{-1}$. For the aftershear portion of the AGT2 and the GGT2, the velocity increases in the level flight branch and is nearly constant in the ascending flight branch; at the final point, the correct quasi-steady value of the velocity is reached. These properties of the AGT2 and the GGT2 are consistent with the analogous properties of the OT2.

(iv) For strong-to-severe windshears, the functions $\gamma(t)$ of the AGT2 and the GGT2 resemble the function $\gamma(t)$ of the OT2. For the shear portion of the AGT2 and the GGT2, the path inclination is negative in descending flight; then, it switches to a slightly positive value (to compensate for downdraft effects). For the aftershear portion of the AGT2 and the GGT2, the path inclination is almost zero, while the velocity increases in nearly horizontal flight; then, the path inclination increases toward the final quasi-steady value, while the velocity is almost constant. These properties of the AGT2 and the GGT2 are consistent with the analogous properties of the OT2.

(v) For strong-to-severe windshears, the functions $\alpha(t)$ of the AGT2 and the GGT2 resemble the function $\alpha(t)$ of the OT2: the angle of attack exhibits an initial decrease, followed by a gradual, sustained increase; the peak value of the angle of attack is achieved near the end of the shear. For the aftershear portion of the AGT2 and the GGT2, the angle of attack decreases as the velocity increases in nearly horizontal flight; in the neighborhood of the final point, a final adjustment in the angle of attack takes place, consistently with the need for recovering the final quasi-steady value of the path inclination.

It must be noted that the function $\alpha(t)$ of the OT2 is much smoother than the functions $\alpha(t)$ of the AGT2 and the GGT2. For both the AGT2

and the GGT2, relatively large oscillations of the angle of attack occur near the points of switch from descent guidance to recovery guidance to level flight guidance to ascent guidance. These oscillations can be reduced by employing some more sophisticated form of feedback control than the simple proportional feedback control considered here.

11. Stability Analysis

In Sections 8-9, we introduced the acceleration guidance scheme and the gamma guidance scheme for quasi-steady flight to quasi-steady flight transition in the abort landing maneuver in a windshear. Both guidance schemes include shear guidance (descent guidance followed by recovery guidance) and aftershear guidance (level flight guidance followed by ascent guidance). Here, we focus our attention on the aftershear guidance. As explained, the level flight guidance is designed to achieve almost complete velocity recovery; the ascent guidance is designed to achieve almost complete restoration of the desired final quasi-steady state.

With reference to the ascent guidance, the feedback control law is given by

$$(AG) \quad \alpha - \tilde{\alpha}(V) = -K(\dot{h} - \dot{h}_r), \quad (40a)$$

or

$$(GG) \quad \alpha - \tilde{\alpha}(V) = -K(\gamma_e - \gamma_{er}), \quad (40b)$$

with the following understanding: Eq. (40a) applies to the acceleration guidance scheme and Eq. (40b) applies to the gamma guidance scheme. The objective of the feedback control law (40) is twofold: (i) to increase steadily the path inclination (hence, the rate of climb) from about zero to the final quasi-steady value, while maintaining the velocity nearly constant; and (ii) to keep the quasi-steady state after it is reached. These objectives can be reached by proper selection of the gain coefficient K . In this section, we present two methods for the determination of K : (a) eigenvalue analysis and (b) direct optimization.

Eigenvalue Analysis. We refer to the ascent portion of the trajectory and we observe that, in the absence of shear, the dynamical equations (2) simplify to

$$\dot{V} = (T/m) \cos(\alpha + \delta) - D/m - g \sin \gamma, \quad (41a)$$

$$\dot{\gamma} = (T/mV) \sin(\alpha + \delta) + L/mV - (g/V) \cos \gamma. \quad (41b)$$

We note that the power setting is at the level $\beta = 1$ and the lift coefficient is in the linear range. Hence, Eqs. (10)–(12) simplify to

$$T = A_0 + A_1 V + A_2 V^2, \tag{42a}$$

$$D = (1/2)\rho S V^2 (B_0 + B_1 \alpha + B_2 \alpha^2), \tag{42b}$$

$$L = (1/2)\rho S V^2 (C_0 + C_1 \alpha). \tag{42c}$$

Therefore, upon combining Eqs. (41)–(42), we obtain the relations

$$\dot{V} = \phi(V, \gamma, \alpha), \tag{43a}$$

$$\dot{\gamma} = \psi(V, \gamma, \alpha), \tag{43b}$$

in which the functions ϕ, ψ are defined by

$$\begin{aligned} \phi = & [(A_0 + A_1 V + A_2 V^2)/m] \cos(\alpha + \delta) \\ & - (\rho S V^2 / 2m)(B_0 + B_1 \alpha + B_2 \alpha^2) - g \sin \gamma, \end{aligned} \tag{44a}$$

$$\begin{aligned} \psi = & [(A_0 + A_1 V + A_2 V^2) / m V] \sin(\alpha + \delta) \\ & + (\rho S V / 2m)(C_0 + C_1 \alpha) - (g / V) \cos \gamma. \end{aligned} \tag{44b}$$

For stability analyses, the linearized form of Eqs. (43) is employed:

$$\Delta \dot{V} = \phi_v \Delta V + \phi_\gamma \Delta \gamma + \phi_\alpha \Delta \alpha, \tag{45a}$$

$$\Delta \dot{\gamma} = \psi_v \Delta V + \psi_\gamma \Delta \gamma + \psi_\alpha \Delta \alpha, \tag{45b}$$

in which the derivatives $\phi_v, \phi_\gamma, \phi_\alpha$ and $\psi_v, \psi_\gamma, \psi_\alpha$ are given by

$$\begin{aligned} \phi_v = & [(A_1 + 2A_2 V) / m] \cos(\alpha + \delta) \\ & - (\rho S V / m)(B_0 + B_1 \alpha + B_2 \alpha^2), \end{aligned} \tag{46a}$$

$$\phi_\gamma = -g \cos \gamma, \tag{46b}$$

$$\begin{aligned} \phi_\alpha = & -[(A_0 + A_1 V + A_2 V^2) / m] \sin(\alpha + \delta) \\ & - (\rho S V^2 / 2m)(B_1 + 2B_2 \alpha), \end{aligned} \tag{46c}$$

and

$$\begin{aligned} \psi_v = & [(-A_0 / V^2 + A_2) / m] \sin(\alpha + \delta) \\ & + (\rho S / 2m)(C_0 + C_1 \alpha) + (g / V^2) \cos \gamma, \end{aligned} \tag{47a}$$

$$\psi_\gamma = (g / V) \sin \gamma, \tag{47b}$$

$$\psi_\alpha = [(A_0 + A_1 V + A_2 V^2) / m V] \cos(\alpha + \delta) + (\rho S V / 2m) C_1. \tag{47c}$$

Here, $\Delta V, \Delta \gamma, \Delta \alpha$ denote the changes of the velocity, the path inclination,

and the angle of attack with respect to some assumed nominal values (the desired quasi-steady values at the final point).

Let the feedback control form of the acceleration guidance law (40a) and the gamma guidance law (40b) be rewritten in the general form

$$\alpha = \tilde{\alpha}(V) - K\omega(V, \gamma), \quad (48)$$

where

$$(AG) \quad \omega = \dot{h} - \dot{h}_r = V \sin \gamma - \dot{h}_r, \quad (49a)$$

or

$$(GG) \quad \omega = \gamma_e - \gamma_{er} \cong \gamma - \gamma_r. \quad (49b)$$

Upon linearization and upon neglecting the contribution due to the fact that the nominal angle of attack depends on the velocity, Eq. (48) yields

$$\Delta\alpha = -K[\omega_v\Delta V + \omega_\gamma\Delta\gamma], \quad (50)$$

where

$$(AG) \quad \omega_v = \sin \gamma, \quad \omega_\gamma = V \cos \gamma, \quad (51a)$$

or

$$(GG) \quad \omega_v = 0, \quad \omega_\gamma = 1. \quad (51b)$$

The next step is to combine the linearized equations (45) and (50) to obtain

$$\Delta\dot{V} = (\phi_v - K\phi_\alpha\omega_v)\Delta V + (\phi_\gamma - K\phi_\alpha\omega_\gamma)\Delta\gamma, \quad (52a)$$

$$\Delta\dot{\gamma} = (\psi_v - K\psi_\alpha\omega_v)\Delta V + (\psi_\gamma - K\psi_\alpha\omega_\gamma)\Delta\gamma. \quad (52b)$$

These equations can be rewritten in the form

$$\begin{bmatrix} \Delta\dot{V} \\ \Delta\dot{\gamma} \end{bmatrix} = \begin{bmatrix} M_{11} & M_{12} \\ M_{21} & M_{22} \end{bmatrix} \begin{bmatrix} \Delta V \\ \Delta\gamma \end{bmatrix}, \quad (53)$$

where

$$M_{11} = \phi_v - K\phi_\alpha\omega_v, \quad (54a)$$

$$M_{12} = \phi_\gamma - K\phi_\alpha\omega_\gamma, \quad (54b)$$

$$M_{21} = \psi_v - K\psi_\alpha\omega_v, \quad (54c)$$

$$M_{22} = \psi_\gamma - K\psi_\alpha\omega_\gamma. \quad (54d)$$

The general solution of (53) can be written as

$$\begin{aligned} \begin{bmatrix} \Delta V \\ \Delta \gamma \end{bmatrix} &= c_1 \begin{bmatrix} E_{11} \\ E_{21} \end{bmatrix} \exp[-\lambda_1(t - t_*)] \\ &+ c_2 \begin{bmatrix} E_{12} \\ E_{22} \end{bmatrix} \exp[-\lambda_2(t - t_*)], \end{aligned} \tag{55}$$

where $-\lambda_1$ and $-\lambda_2$ denote the eigenvalues of the matrix in (53) and $[E_{11}, E_{21}]^T$ and $[E_{12}, E_{22}]^T$ denote the corresponding eigenvectors. The symbol t_* denotes the time at which the ascent guidance begins.

Numerical experiments show that, as the gain coefficient K increases, λ_1 increases, λ_2 approaches zero, and the ratio E_{12}/E_{22} approaches a small value. Assume now that, at the beginning of the ascent guidance,

$$\Delta V(t_*) = 0, \quad \Delta \gamma(t_*) \neq 0. \tag{56}$$

This implies that $c_1 \equiv 0$, so that Eqs. (55) simplify to

$$\begin{bmatrix} \Delta V \\ \Delta \gamma \end{bmatrix} \equiv c_2 \begin{bmatrix} 0 \\ E_{22} \end{bmatrix} \exp[-\lambda_2(t - t_*)]; \tag{57}$$

therefore,

$$\Delta V = 0, \quad \text{for all } t, \tag{58a}$$

$$\Delta \gamma \rightarrow 0, \quad \text{for } t \rightarrow \tau, \tag{58b}$$

so that

$$V = V_\tau, \quad \text{for all } t, \tag{59a}$$

$$\gamma \rightarrow \gamma_\tau, \quad \text{for } t \rightarrow \tau. \tag{59b}$$

Clearly, the above analysis shows that large values of the gain coefficient should be used. However, as K increases, both the changes of α and the changes of $\dot{\alpha}$ become larger, with the following consequence: the control bounds in Ineqs. (6) become saturated. Thus, in practice, K must be chosen as a compromise between the need for approaching quickly the quasi-steady state and the need for avoiding too frequent saturations of the control bounds.

Direct Optimization. An alternative way of selecting the gain coefficient is based on an optimization procedure. We consider the minimization of the performance index

$$I = \int_{t_*}^{\tau} [(\Delta V)^2 + L_1(\Delta \gamma)^2 + L_2(\Delta \alpha)^2] dt, \tag{60}$$

with respect to the functions $\Delta V(t)$, $\Delta \gamma(t)$, $\Delta \alpha(t)$ and the parameter K which satisfy the constraints (45) and (50). In the minimization process, the initial values $\Delta V(t_*)$, $\Delta \gamma(t_*)$, $\Delta \alpha(t_*)$ are given and the final values $\Delta V(\tau)$, $\Delta \gamma(\tau)$, $\Delta \alpha(\tau)$ are required to approach zero. The symbols L_1 and L_2 denote weighting coefficients.

Of particular importance is the weighting coefficient L_2 . If L_2 is small, ΔV , $\Delta \gamma$ are brought to zero rapidly; however, K is large and $\Delta \alpha$ is large, so that the bounds on α and $\dot{\alpha}$ become saturated. If L_2 is large, ΔV , $\Delta \gamma$ are brought to zero slowly; however, K is small and $\Delta \alpha$ is small, so that the bounds on α and $\dot{\alpha}$ do not become saturated. Once more, the value of L_2 (hence, the value of K) must be chosen as a compromise between the need for approaching quickly the quasi-steady state and the need for avoiding too frequent saturations of the control bounds.

12. Conclusions

This paper is concerned with the optimal transition and the near-optimum guidance of an aircraft from quasi-steady flight to quasi-steady flight in a windshear. The abort landing problem is considered with reference to flight in a vertical plane. In addition to the horizontal shear, the presence of a downdraft is considered.

It is assumed that a transition from descending flight to ascending flight is desired; that the initial state corresponds to quasi-steady flight with absolute path inclination of -3.0 deg; and that the final path inclination corresponds to quasi-steady steepest climb. Also, it is assumed that, as soon as the shear is detected, the power setting is increased at a constant time rate until maximum power setting is reached; afterward, the power setting is held constant. Hence, the only control is the angle of attack. Inequality constraints are imposed on both the angle of attack and its time derivative.

First, trajectory optimization is considered. The optimal transition problem is formulated as a Chebyshev problem of optimal control: the performance index being minimized is the peak value of the modulus of the difference between the instantaneous altitude and a reference value, assumed constant. By suitable transformations, the Chebyshev problem is converted into a Bolza problem. Then, the Bolza problem is solved employing the dual sequential gradient-restoration algorithm (DSGRA) for optimal control problems.

Two types of optimal trajectories are studied, depending on the conditions desired at the final point. Type 1 is concerned with gamma recovery (recovery of the value of the relative path inclination corresponding to quasi-steady steepest climb). Type 2 is concerned with quasi-steady flight

recovery (recovery of the values of the relative path inclination, the relative velocity, and the relative angle of attack corresponding to quasi-steady steepest climb). Both the Type 1 trajectory and the Type 2 trajectory include three branches: descending flight, nearly horizontal flight, and ascending flight. Also, for both the Type 1 trajectory and the Type 2 trajectory, descending flight takes place in the shear portion of the trajectory; horizontal flight takes place partly in the shear portion and partly in the aftershear portion of the trajectory; and ascending flight takes place in the aftershear portion of the trajectory. While the Type 1 trajectory and the Type 2 trajectory are nearly the same in the shear portion, they diverge to a considerable degree in the aftershear portion of the trajectory.

Next, trajectory guidance is considered. Two guidance schemes are developed so as to achieve near-optimum transition from quasi-steady descending flight to quasi-steady ascending flight: acceleration guidance (based on the relative acceleration) and gamma guidance (based on the absolute path inclination).

The guidance schemes for quasi-steady flight recovery in abort landing include two parts in sequence: shear guidance and aftershear guidance. The shear guidance is based on the result that the shear portion of the trajectory depends only mildly on the boundary conditions. Therefore, any of the guidance schemes already developed for Type 1 trajectories can be employed for Type 2 trajectories (descent guidance followed by recovery guidance). The aftershear guidance is based on the result that the aftershear portion of the trajectory depends strongly on the boundary conditions; therefore, the guidance schemes developed for Type 1 trajectories cannot be employed for Type 2 trajectories. For Type 2 trajectories, the aftershear guidance includes level flight guidance followed by ascent guidance. The level flight guidance is designed to achieve almost complete velocity recovery; the ascent guidance is designed to achieve the desired final quasi-steady state.

The numerical results show that the guidance schemes for quasi-steady flight recovery yield a transition from quasi-steady flight to quasi-steady flight which is close to that of the optimal trajectory, allows the aircraft to achieve the final quasi-steady state, and has good stability properties.

References

1. FUJITA, T. T., *The Downburst*, Department of Geophysical Sciences, University of Chicago, Chicago, Illinois, 1985.
2. ANONYMOUS, N. N., *Aircraft Accident Report: Pan American World Airways, Clipper 759, Boeing 727-235, N4737, New Orleans International Airport, Kenner, Louisiana, July 9, 1982*, Report No. NTSB-AAR-8302, National Transportation Safety Board, Washington, DC, 1983.

3. ANONYMOUS, N. N., *Aircraft Accident Report: Delta Air Lines, Lockheed L-1011-3851, N726DA, Dallas-Fort Worth International Airport, Texas, August 2, 1985*, Report No. NTSB-AAR-8605, National Transportation Safety Board, Washington, DC, 1986.
4. FUJITA, T. T., *DFW Microburst*, Department of Geophysical Sciences, University of Chicago, Chicago, Illinois, 1986.
5. GORNEY, J. L., *An Analysis of the Delta 191 Windshear Accident*, Paper No. AIAA-87-0626, AIAA 25th Aerospace Sciences Meeting, Reno, Nevada, 1987.
6. ANONYMOUS, N. N., *Flight Path Control in Windshear*, Boeing Airliner, pp. 1-12, January-March 1985.
7. ANONYMOUS, N. N., *Windshear Training Aid, Vols. 1 and 2*, Federal Aviation Administration, Washington, DC, 1987.
8. BRAY, R. S., *Aircraft Performance and Control in Downburst Windshear*, Paper No. SAE-86-1698, SAE Aerospace Technology Conference and Exposition, Long Beach, California, 1986.
9. MIELE, A., WANG, T., TZENG, C. Y., and MELVIN, W. W., *Transformation Techniques for Minimax Optimal Control Problems and Their Application to Optimal Flight Trajectories in a Windshear: Optimal Abort Landing Trajectories*, Paper No. IFAC-87-9221, IFAC 10th World Congress, Munich, Germany, 1987.
10. MIELE, A., WANG, T., TZENG, C. Y., and MELVIN, W. W., *Optimization and Guidance of Abort Landing Trajectories in a Windshear*, Paper No. AIAA-87-2341, AIAA Guidance, Navigation, and Control Conference, Monterey, California, 1987.
11. MIELE, A., WANG, T., and MELVIN, W. W., *Acceleration, Gamma, and Theta Guidance Schemes for Abort Landing Trajectories in the Presence of Windshear*, Rice University, Aero-Astronautics Report No. 223, 1987.
12. MIELE, A., WANG, T., and MELVIN, W. W., *Optimization and Acceleration Guidance of Flight Trajectories in a Windshear*, Journal of Guidance, Control, and Dynamics, Vol. 10, No. 4, pp. 368-377, 1987.
13. MIELE, A., WANG, T., and MELVIN, W. W., *Optimization and Gamma/Theta Guidance of Flight Trajectories in a Windshear*, Paper No. ICAS-86-564, 15th Congress of the International Council of the Aeronautical Sciences, London, England, 1986.
14. MIELE, A., WANG, T., and MELVIN, W. W., *Optimal Take-Off Trajectories in the Presence of Windshear*, Journal of Optimization Theory and Applications, Vol. 49, No. 1, pp. 1-45, 1986.
15. MIELE, A., WANG, T., and MELVIN, W. W., *Guidance Strategies for Near-Optimum Take-Off Performance in a Windshear*, Journal of Optimization Theory and Applications, Vol. 50, No. 1, pp. 1-47, 1986.
16. MIELE, A., WANG, T., MELVIN, W. W., and BOWLES, R. L., *Maximum Survival Capability of an Aircraft in a Severe Windshear*, Journal of Optimization Theory and Applications, Vol. 53, No. 2, pp. 181-217, 1987.
17. MIELE, A., WANG, T., and MELVIN, W. W., *Quasi-Steady Flight to Quasi-Steady Flight Transition in a Windshear: Trajectory Optimization and Guidance*, Journal of Optimization Theory and Applications, Vol. 54, No. 2, pp. 203-240, 1987.

18. MIELE, A., *Primal-Dual Sequential Gradient-Restoration Algorithms for Optimal Control Problems and Their Application to Flight in a Windshear*, Proceedings of the International Conference on Optimization Techniques and Applications, Edited by K. L. Teo et al., Kent Ridge, Singapore, pp. 53-94, 1987.
19. MIELE, A., WANG, T., WANG, H., and MELVIN, W. W., *Optimal Penetration Landing Trajectories in the Presence of Windshear*, Rice University, Aero-Astronautics Report No. 216, 1987.
20. MIELE, A., WANG, T., and MELVIN, W. W., *Penetration Landing Guidance Trajectories in the Presence of Windshear*, Rice University, Aero-Astronautics Report No. 218, 1987.
21. FROST, W., CHANG, H. P., ELMORE, K. L., and MCCARTHY, J., *Simulated Flight through JAWS Windshear: In-Depth Analysis Results*, Paper No. AIAA-84-0276, AIAA 22nd Aerospace Sciences Meeting, Reno, Nevada, 1984.
22. IVAN, M., *A Ring-Vortex Downburst Model for Flight Simulation*, Journal of Aircraft, Vol. 23, No. 3, pp. 232-236, 1986.
23. ZHU, S., and ETKIN, B., *Model of the Wind Field in a Downburst*, Journal of Aircraft, Vol. 22, No. 7, pp. 595-601, 1985.
24. GONZALEZ, S., and MIELE, A., *Sequential Gradient-Restoration Algorithm for Optimal Control Problems with General Boundary Conditions*, Journal of Optimization Theory and Applications, Vol. 26, No. 3, pp. 395-425, 1978.
25. MIELE, A., *Gradient Algorithms for the Optimization of Dynamic Systems*, Control and Dynamic Systems, Advances in Theory and Application, Edited by C. T. Leondes, Academic Press, New York, New York, Vol. 16, pp. 1-52, 1980.
26. MIELE, A., and WANG, T., *Primal-Dual Properties of Sequential Gradient-Restoration Algorithms for Optimal Control Problems, Part 1, Basic Problem*, Integral Methods in Science and Engineering, Edited by F. R. Payne et al., Hemisphere Publishing Corporation, Washington, DC, pp. 577-607, 1986.
27. MIELE, A., and WANG, T., *Primal-Dual Properties of Sequential Gradient-Restoration Algorithms for Optimal Control Problems, Part 2, General Problem*, Journal of Mathematical Analysis and Applications, Vol. 119, Nos. 1-2, pp. 21-54, 1986.

Table 1. Initial conditions.

Quantity	$\lambda = 0.00$	$\lambda = 1.00$	$\lambda = 1.20$	$\lambda = 1.40$	Units
V_0	239.7	239.7	239.7	239.7	ft sec ⁻¹
γ_{e0}	-3.000	-3.000	-3.000	-3.000	deg
γ_0	-3.000	-2.375	-2.249	-2.124	deg
α_0	7.370	7.353	7.349	7.345	deg
θ_0	4.370	4.978	5.100	5.221	deg
β_0	0.3330	0.3743	0.3825	0.3907	—

Table 2. Final conditions.

Quantity	$\lambda = 0.00$	$\lambda = 1.00$	$\lambda = 1.20$	$\lambda = 1.40$	Units
V_τ	217.8	217.8	217.8	217.8	ft sec ⁻¹
$\gamma_{e\tau}$	7.431	6.045	5.828	5.625	deg
γ_τ	7.431	7.431	7.431	7.431	deg
α_τ	9.517	9.517	9.517	9.517	deg
θ_τ	16.95	16.95	16.95	16.95	deg
β_τ	1.000	1.000	1.000	1.000	—

Table 3. Numerical results, optimal trajectories OT1.

h_0 (ft)	ΔW_x (ft sec ⁻¹)	h_{\min} (ft)	h_τ (ft)	V_τ (ft sec ⁻¹)	γ_τ (deg)	α_τ (deg)
200	100	189.0	596.5	178.9	7.43	12.78
200	120	182.5	483.6	181.3	7.43	12.64
200	140	80.8	379.5	179.3	7.43	11.85
600	100	499.4	835.0	179.3	7.43	13.41
600	120	376.1	699.9	179.8	7.43	13.31
600	140	251.0	571.4	183.1	7.43	13.02
1000	100	720.4	1059.5	178.4	7.43	13.67
1000	120	559.4	898.9	178.2	7.43	13.74
1000	140	407.3	750.3	179.6	7.43	13.83

Table 4. Numerical results, optimal trajectories OT2.

h_0 (ft)	ΔW_x (ft sec ⁻¹)	h_{\min} (ft)	h_τ (ft)	V_τ (ft sec ⁻¹)	γ_τ (deg)	α_τ (deg)
200	100	189.0	421.0	217.8	7.43	9.52
200	120	175.5	311.9	217.8	7.43	9.52
200	140	73.0	215.7	217.8	7.43	9.52
600	100	503.6	656.7	217.8	7.43	9.52
600	120	371.6	522.1	217.8	7.43	9.52
600	140	247.9	402.0	217.8	7.43	9.52
1000	100	717.7	885.6	217.8	7.43	9.52
1000	120	556.9	713.1	217.8	7.43	9.52
1000	140	402.1	570.9	217.8	7.43	9.52

Table 5. Numerical results, acceleration guidance trajectories AGT2.

h_0 (ft)	ΔW_x (ft sec ⁻¹)	h_{\min} (ft)	h_τ (ft)	V_τ (ft sec ⁻¹)	γ_τ (deg)	α_τ (deg)
200	100	185.6	179.6	218.3	7.48	9.51
200	120	141.2	171.2	218.2	7.47	9.54
200	140	-28.7	166.5	217.5	7.53	9.60
600	100	407.3	195.5	218.4	7.52	9.45
600	120	291.5	193.0	218.0	7.54	9.50
600	140	188.7	189.7	217.8	7.54	9.52
1000	100	604.8	199.1	218.5	7.52	9.44
1000	120	480.2	192.2	218.3	7.53	9.46
1000	140	352.2	186.2	217.8	7.54	9.53

Table 6. Numerical results, gamma guidance trajectories GGT2.

h_0 (ft)	ΔW_x (ft sec ⁻¹)	h_{min} (ft)	h_r (ft)	V_r (ft sec ⁻¹)	γ_r (deg)	α_r (deg)
200	100	181.0	198.9	217.6	7.41	9.55
200	120	177.3	175.9	217.4	7.40	9.58
200	140	-18.9	162.3	216.6	7.34	9.70
600	100	453.0	188.6	217.5	7.41	9.56
600	120	348.3	181.6	217.4	7.40	9.57
600	140	234.2	178.6	217.3	7.39	9.59
1000	100	638.0	193.5	217.5	7.41	9.56
1000	120	520.0	183.4	217.3	7.40	9.59
1000	140	387.0	176.2	217.3	7.39	9.59

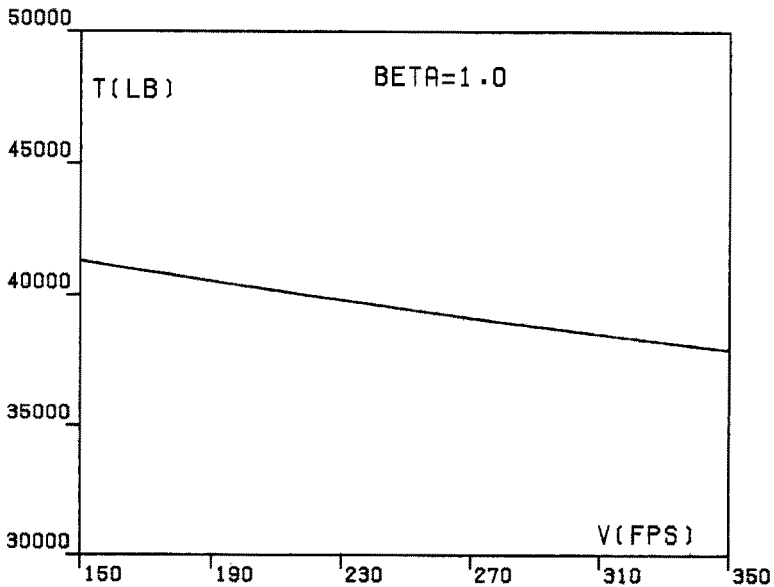


Fig. 1A. Thrust T_* versus velocity V for the Boeing B-727 aircraft powered by three JT8D-17 turbofan engines (maximum power setting, sea-level altitude, ambient temperature = 100 deg F).

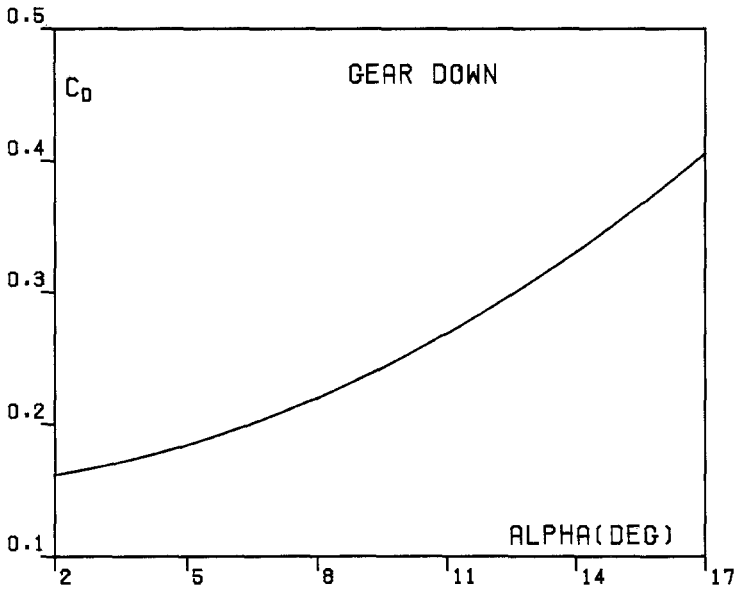


Fig. 1B. Drag coefficient C_D versus angle of attack α for the Boeing B-727 aircraft (gear down, flap setting $\delta_F = 30$ deg).

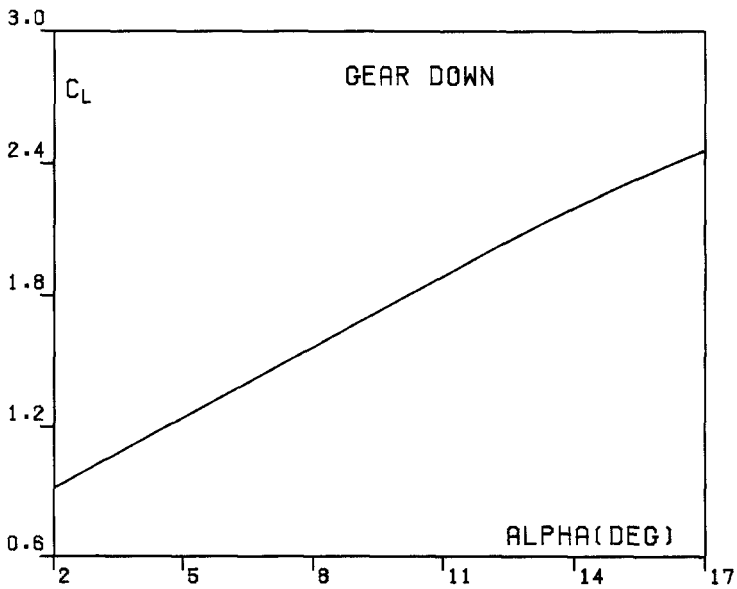


Fig. 1C. Lift coefficient C_L versus angle of attack α for the Boeing B-727 aircraft (gear down, flap setting $\delta_F = 30$ deg).

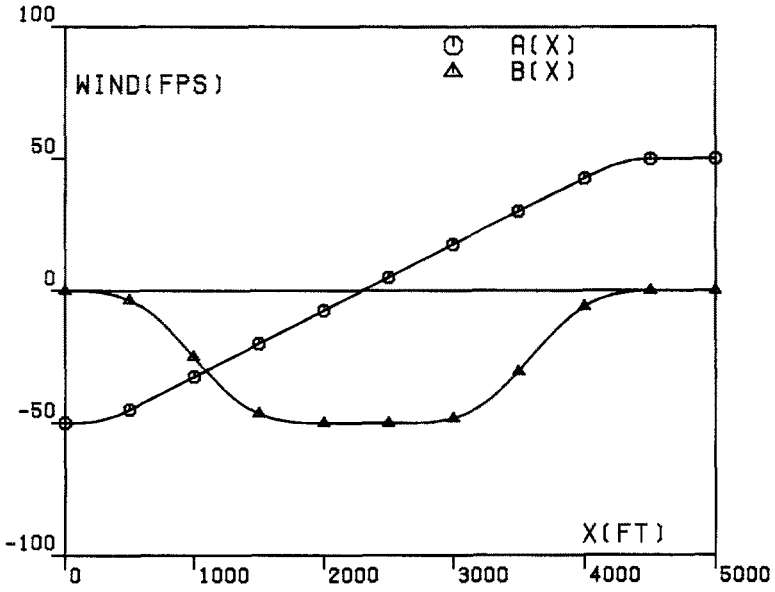


Fig. 2. Horizontal wind function $A(x)$ and vertical wind function $B(x)$.

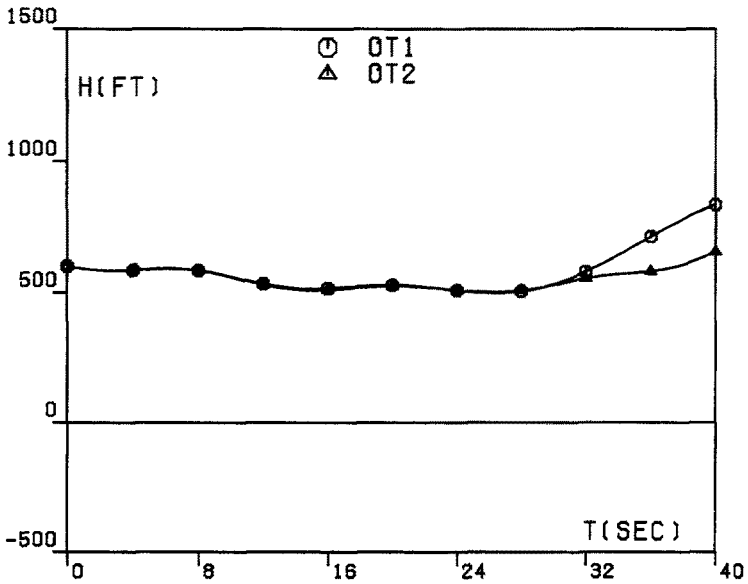


Fig. 3A. Optimal trajectories OT1 and OT2, $h_0 = 600$ ft, $\Delta W_x = 100$ ft sec⁻¹: altitude h versus time t .

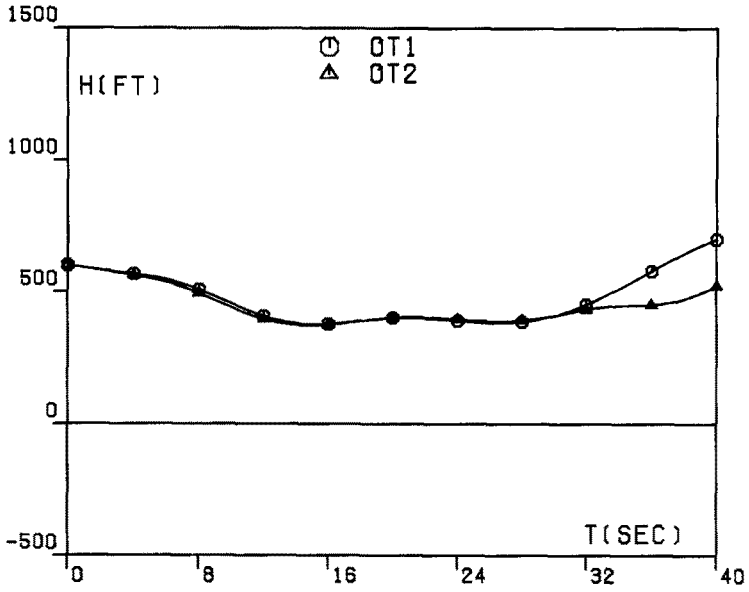


Fig. 3B. Optimal trajectories OT1 and OT2, $h_0 = 600$ ft, $\Delta W_x = 120$ ft sec⁻¹: altitude h versus time t .

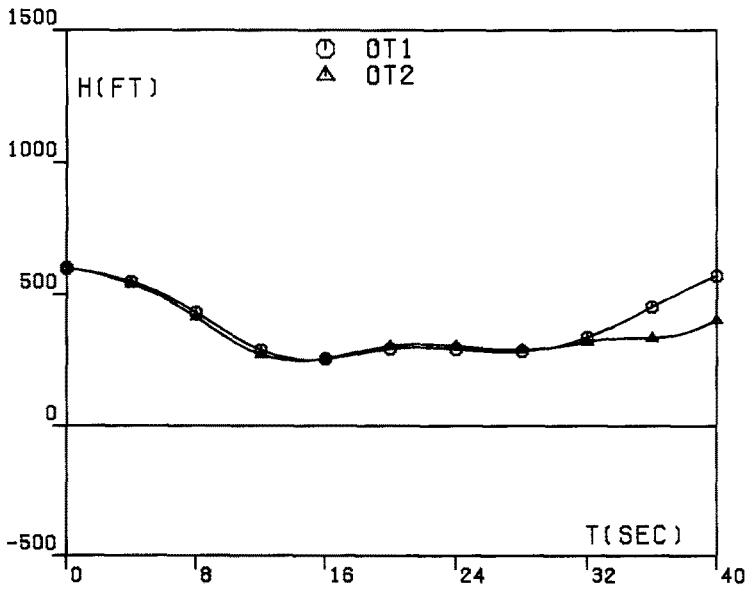


Fig. 3C. Optimal trajectories OT1 and OT2, $h_0 = 600$ ft, $\Delta W_x = 140$ ft sec⁻¹: altitude h versus time t .

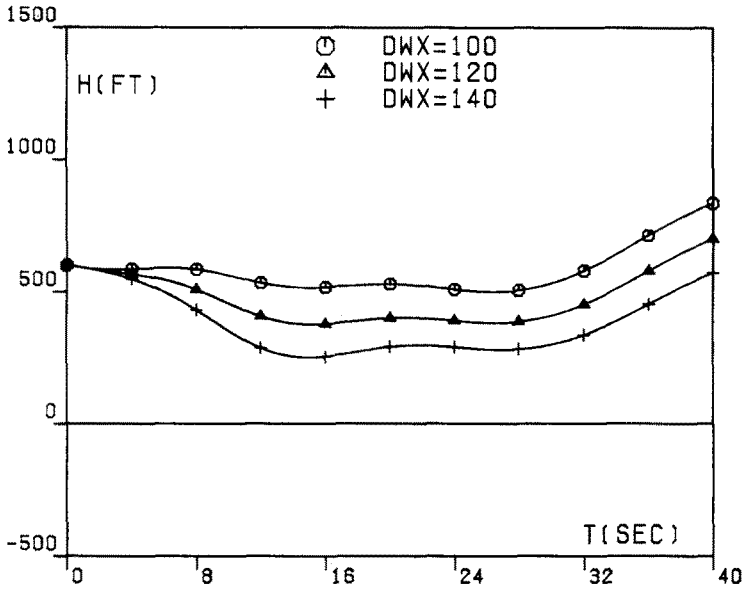


Fig. 4A. Optimal trajectories OT1, $h_0 = 600$ ft: altitude h versus time t .

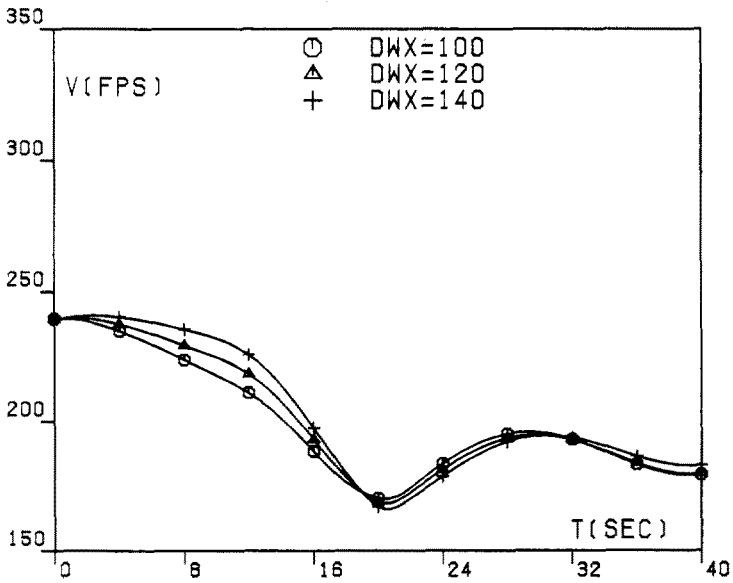


Fig. 4B. Optimal trajectories OT1, $h_0 = 600$ ft: velocity V versus time t .

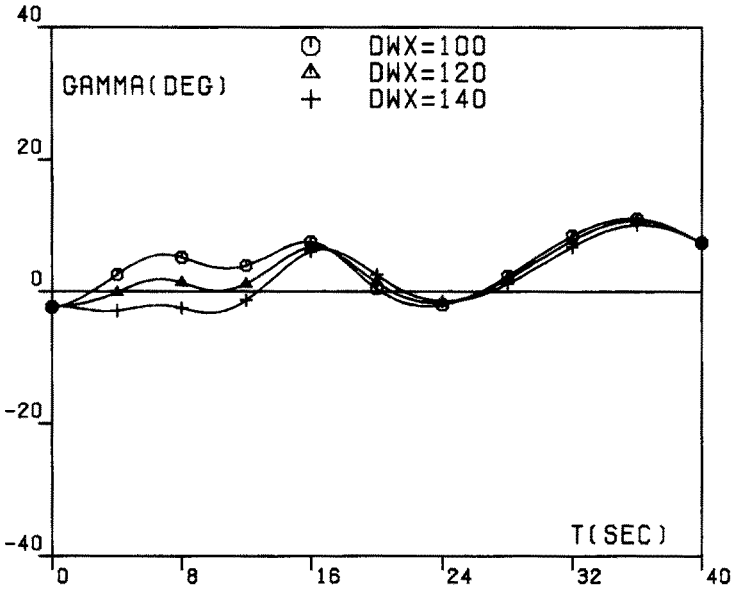


Fig. 4C. Optimal trajectories OT1, $h_0 = 600$ ft: path inclination γ versus time t .

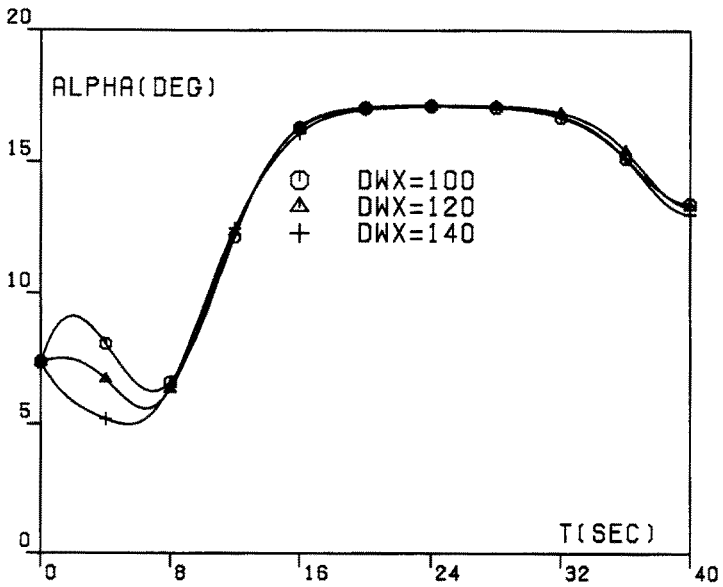


Fig. 4D. Optimal trajectories OT1, $h_0 = 600$ ft: angle of attack α versus time t .

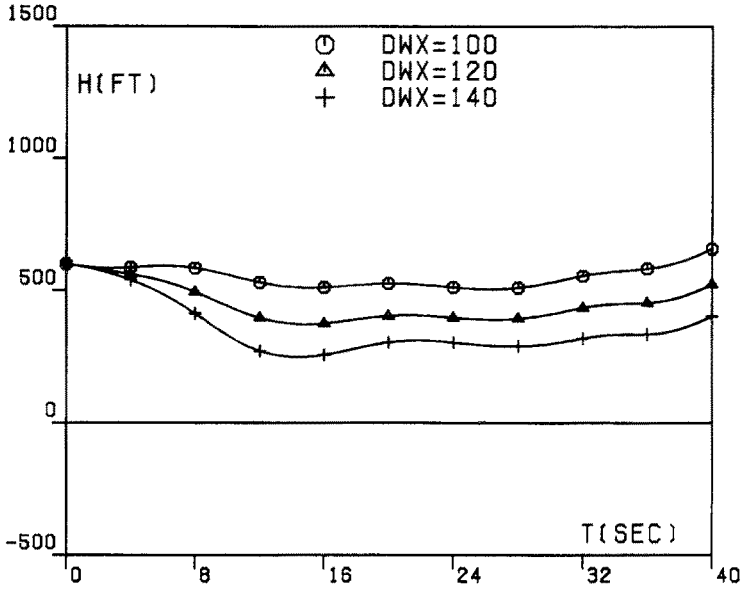


Fig. 5A. Optimal trajectories OT2, $h_0 = 600$ ft: altitude h versus time t .

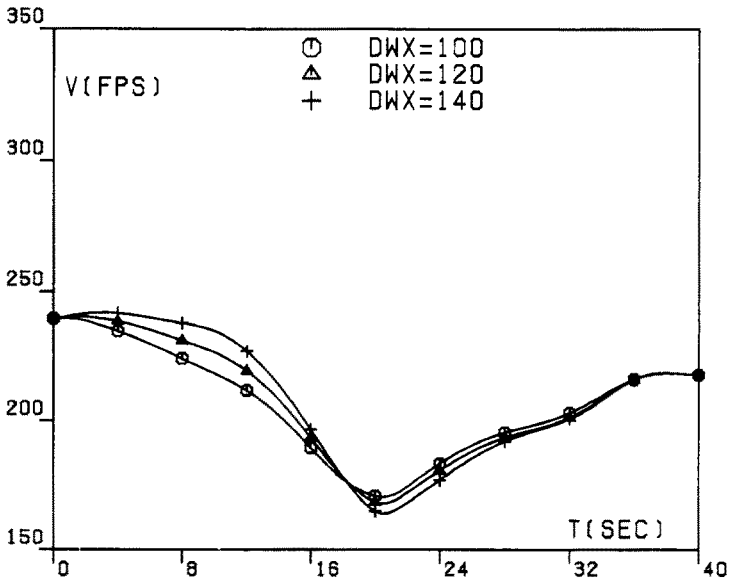


Fig. 5B. Optimal trajectories OT2, $h_0 = 600$ ft: velocity V versus time t .

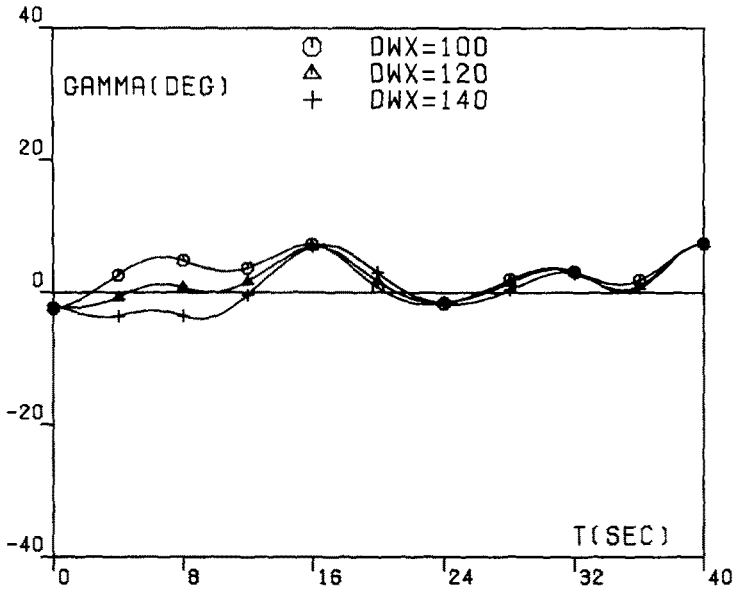


Fig. 5C. Optimal trajectories OT2, $h_0 = 600$ ft: path inclination γ versus time t .

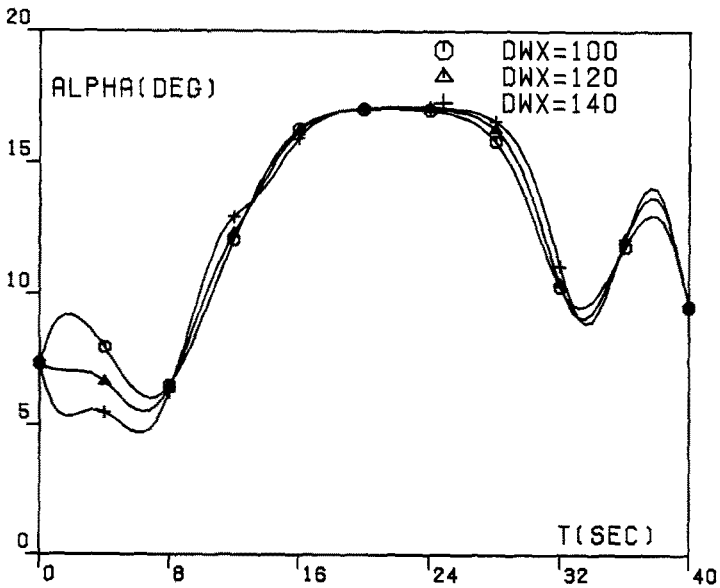


Fig. 5D. Optimal trajectories OT2, $h_0 = 600$ ft: angle of attack α versus time t .

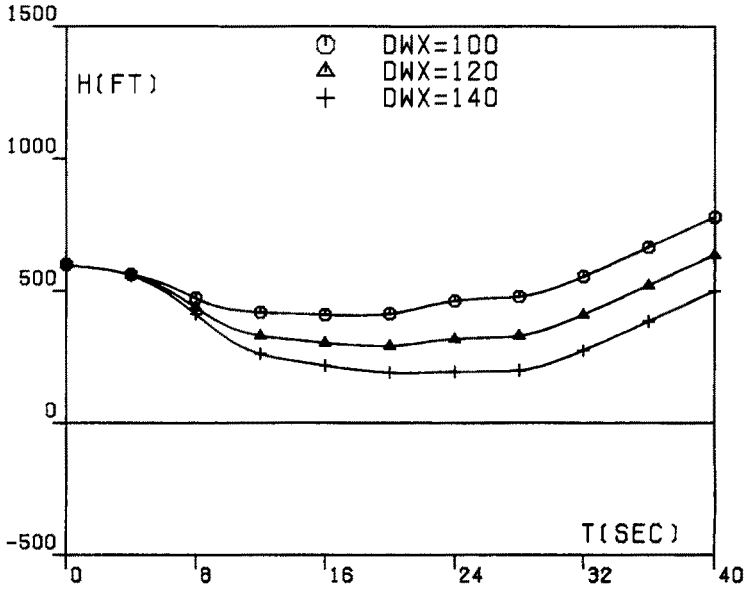


Fig. 6A. Acceleration guidance trajectories AGT2, $h_0 = 600$ ft: altitude h versus time t .

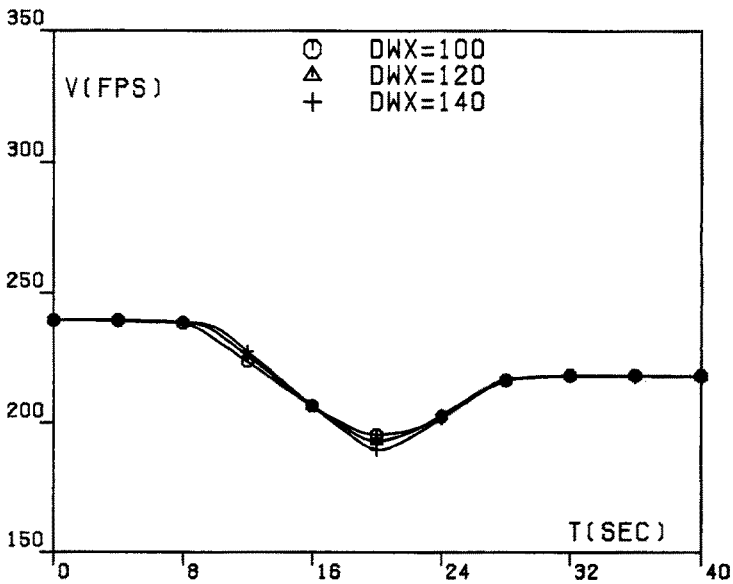


Fig. 6B. Acceleration guidance trajectories AGT2, $h_0 = 600$ ft: velocity V versus time t .

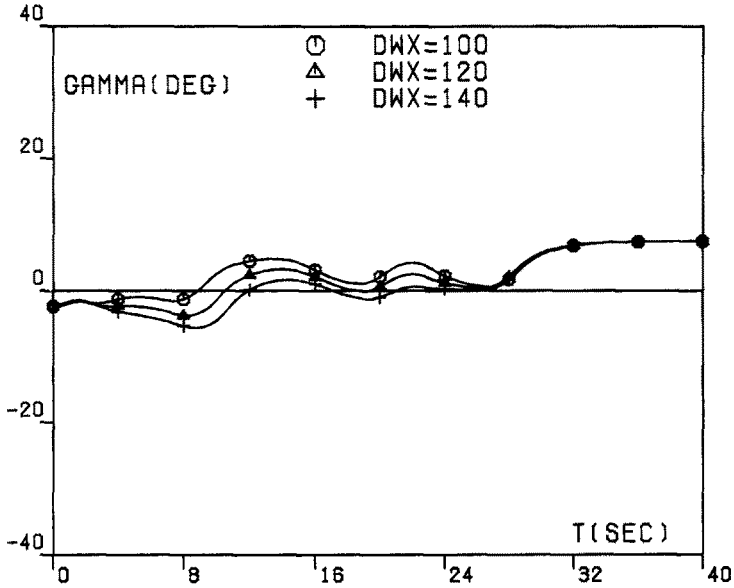


Fig. 6C. Acceleration guidance trajectories AGT2, $h_0 = 600$ ft: path inclination γ versus time t .

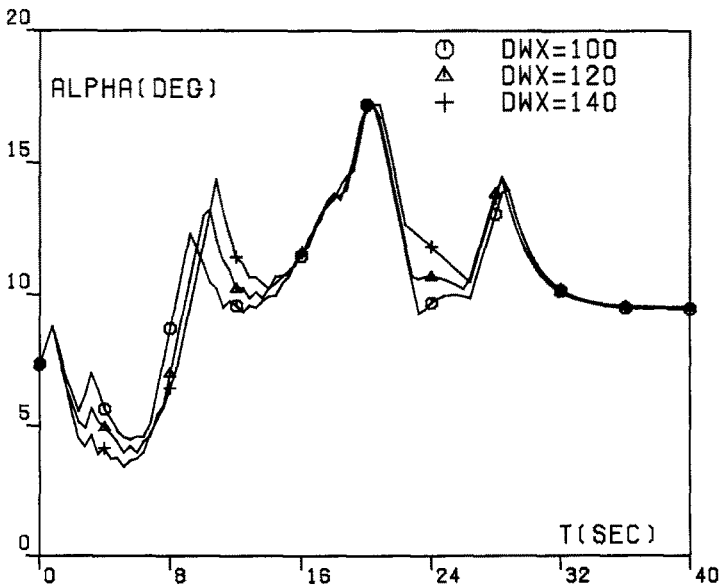


Fig. 6D. Acceleration guidance trajectories AGT2, $h_0 = 600$ ft: angle of attack α versus time t .

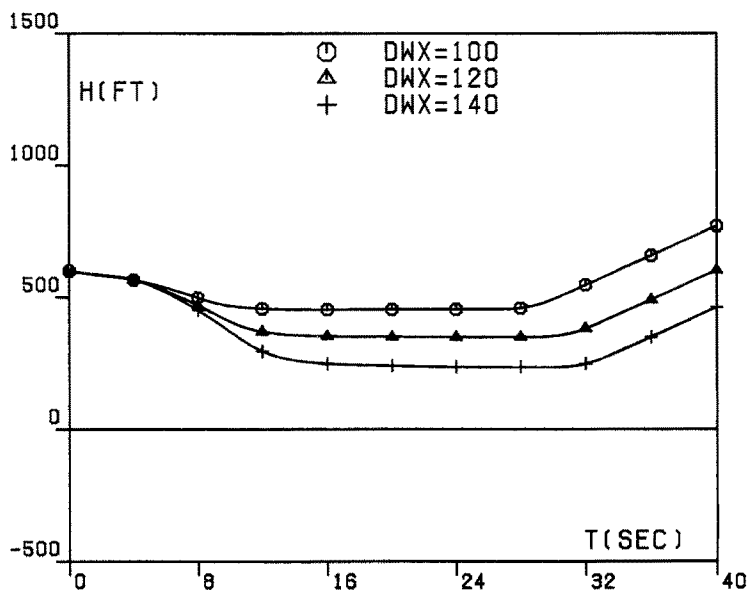


Fig. 7A. Gamma guidance trajectories GGT2, $h_0 = 600$ ft: altitude h versus time t .

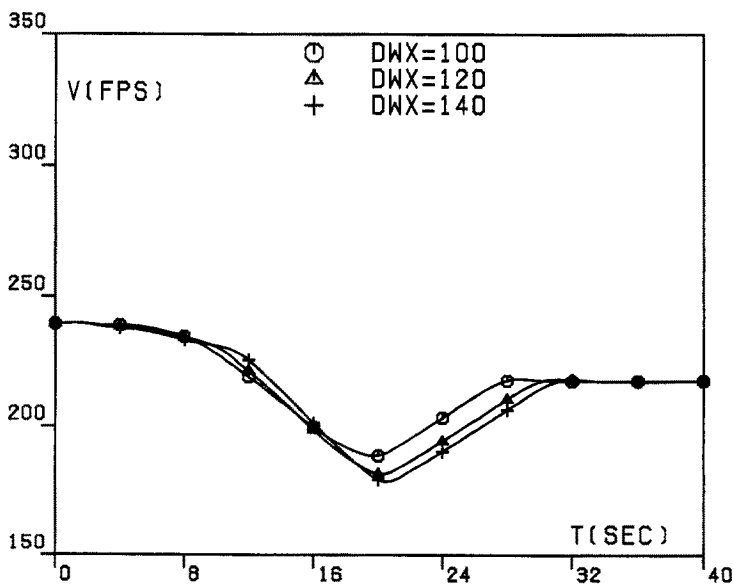


Fig. 7B. Gamma guidance trajectories GGT2, $h_0 = 600$ ft: velocity V versus time t .

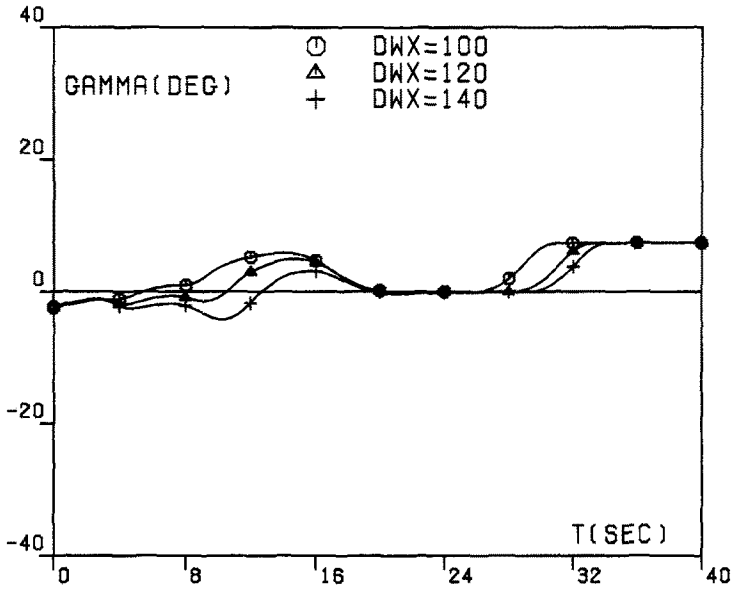


Fig. 7C. Gamma guidance trajectories GGT2, $h_0 = 600$ ft: path inclination γ versus time t .

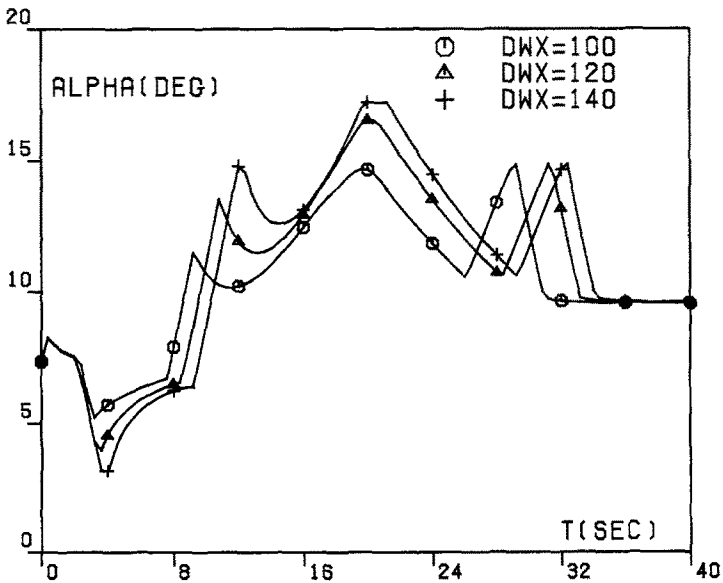


Fig. 7D. Gamma guidance trajectories GGT2, $h_0 = 600$ ft: angle of attack α versus time t .